Article

Translation-dependent degradation of *cas12* mRNA triggered by an anti-CRISPR

https://doi.org/10.1038/s41586-026-10440-8

Received: 19 June 2023

Accepted: 23 March 2026

Published online: 29 April 2026

Check for updates

Nicole D. Marino[1,2]✉, Alexander Talaie[1], Milan Gerovac[3], Jorge L. Rodriguez[2], Andrew D. Schmidt[2], Theresa J. Astmann[2], Héloïse Carion[1], Anya Flood Taylor[2], Jessica Liliedahl[2], Surabhi Haniyur[1], Kristi Zoga[2], Matthew C. Johnson[1], Leandro Buhlmann[4], Kuei-Ho Chen[5,6,7], Sukrit Silas[1,6], Li Yuping[1,8], Yang Zhang[1], Danielle L. Swaney[5,6,7], Jörg Vogel[4,9] & Joseph Bondy-Denomy[1,5]✉

Bacteria encode diverse defence systems, including CRISPR–Cas, to recognize and cleave the DNA of bacteriophages (phages) and other mobile genetic elements[1]. In response, phages encode anti-CRISPR (Acr) proteins that inhibit CRISPR–Cas activity by blocking DNA binding or cleavage[2]. Here we report an unexpected mechanism by which the anti-CRISPR AcrVA2 inhibits Cas12a biogenesis. AcrVA2 binds conserved and functionally important amino acid residues near the Cas12a N-terminus and triggers selective degradation of *cas12a* mRNA as it is translated. Additionally, conserved residues in the AcrVA2 C-terminal domain enable co-sedimentation with ribosomes and polysomes, which is required to achieve targeted co-translational mRNA degradation. The AcrVA2 C-terminal domain is broadly conserved in homologs encoded by diverse mobile genetic elements, typically in hosts that lack *cas12a*, suggesting that these homologues may recognize and downregulate alternative substrates in other bacteria. These findings reveal a novel mechanism for molecular conflict and gene regulation in bacteria.

Most known anti-CRISPRs inhibit CRISPR–Cas cleavage by directly binding to the ribonucleoprotein (RNP) complex and inhibiting target binding or conformational activation, whereas others enzymatically modify the complex[3,4]. For example, the broad-spectrum inhibitor AcrVA1 inactivates Cas12a by cleaving its CRISPR RNA (crRNA)[5,6]. AcrVA1 is encoded next to another Cas12a inhibitor, AcrVA2, that is notably large (approximately 37 kDa) and widely distributed on mobile genetic elements across diverse bacterial taxa[7]. AcrVA2 potently inhibits *Moraxella bovoculi* Cas12a (MbCas12a) in bacteria but not in human cells[7], yet its mechanism has remained unclear. Here we show that AcrVA2 targets a conserved N-terminal motif in diverse Cas12a homologues to interrupt Cas12a biogenesis and trigger selective *cas12a* mRNA degradation.

Downregulation of *cas12a* mRNA

M. bovoculi is not genetically tractable, which limited our ability to investigate the AcrVA2 mechanism in its native host. We therefore engineered *Pseudomonas aeruginosa* PAO1 strains to express plasmid-borne AcrVA2 alongside a chromosomal copy of MbCas12a or *Lachnospiraceae bacterium* Cas12a (LbCas12a), which share 35% amino acid identity and are expressed from different inducible promoters (Fig. 1a). AcrVA2 inhibited phage targeting by both Cas12a homologues (Fig. 1a and Extended Data Fig. 1a) and reduced their protein and mRNA levels despite the divergence in nucleotide sequence (Fig. 1b,c and Extended Data Fig. 1b). The degree to which AcrVA2 and AcrVA2.1 (an orthologue with 84% identity) downregulated MbCas12a and LbCas12a correlated well with their ability to inhibit both orthologues (for example, AcrVA2.1 was less active against LbCas12a). Silent mutations at wobble positions throughout the Mb*cas12a* coding sequence had no effect on AcrVA2-mediated mRNA and protein downregulation (Extended Data Fig. 1c,d), suggesting that AcrVA2 does not recognize a specific nucleotide sequence.

The reduction in *cas12a* mRNA levels was surprising and prompted us to investigate whether AcrVA2 affects additional transcripts. Transcriptomic analysis confirmed that *cas12a* was downregulated by AcrVA2, whereas most other genes were unaffected (Fig. 1d and Extended Data Fig. 2a–d). Closer inspection of the *cas12a* transcripts revealed a strong reduction of reads, particularly towards the 3′ end of the gene (Extended Data Fig. 2e). Together, these findings demonstrate that AcrVA2 specifically downregulates the mRNA of *cas12a* homologues independently of the promoter element and despite divergent nucleotide sequences.

Essential conserved residues in AcrVA2

AcrVA2 lacks recognizable domains and neither its crystal structure nor predicted structure revealed similarity to characterized proteins[8–11]. To identify critical residues required for activity, we generated point mutants in amino acids that are highly conserved across divergent AcrVA2 orthologues. W79A, H286A, R288A and H291A substitutions

[1]Department of Microbiology and Immunology, University of California, San Francisco, San Francisco, CA, USA. [2]Department of Pathobiology, University of Pennsylvania, Philadelphia, PA, USA. [3]Helmholtz Centre for Infection Research, Brunswick, Germany. [4]Institute for Molecular Infection Biology (IMIB), University of Würzburg, Würzburg, Germany. [5]Quantitative Biosciences Institute, University of California, San Francisco, San Francisco, CA, USA. [6]Gladstone Infectious Disease Institute, J. David Gladstone Institutes, San Francisco, CA, USA. [7]Department of Bioengineering and Therapeutic Sciences, University of California, San Francisco, San Francisco, CA, USA. [8]Biozentrum, University of Basel, Basel, Switzerland. [9]Helmholtz Institute for RNA-based Infection Research (HIRI), Helmholtz Centre for Infection Research (HZI), Würzburg, Germany. ✉e-mail: ndmarino@upenn.edu; Joseph.Bondy-Denomy@ucsf.edu

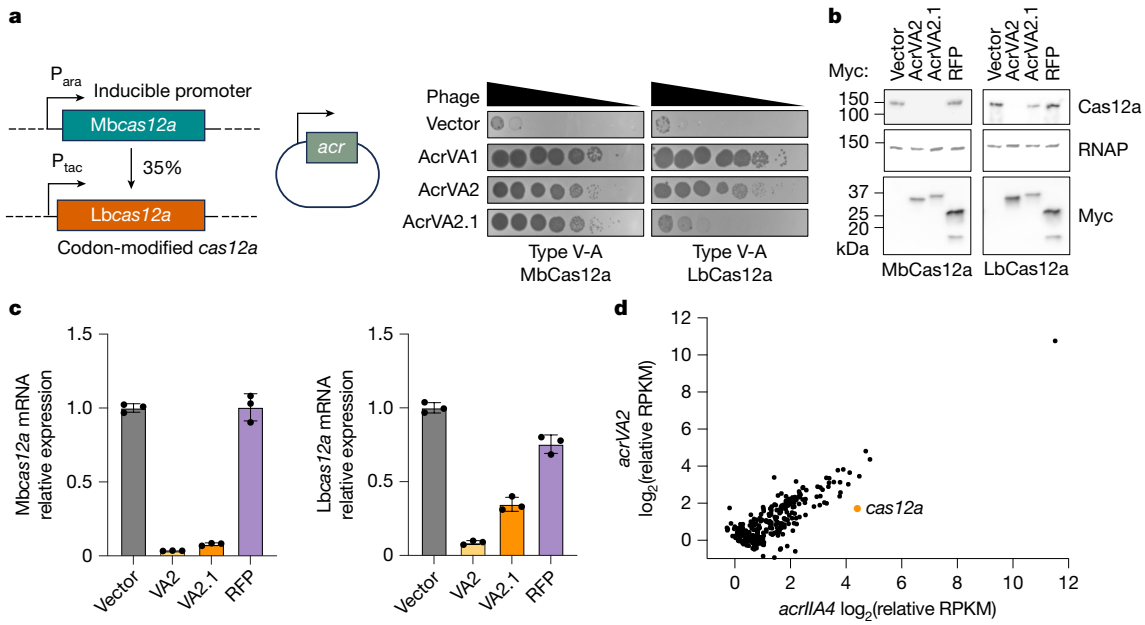


Fig. 1 | AcrVA2 specifically downregulates mRNA and protein of divergent *cas12a* orthologues. a, Schematic of strains engineered to express chromosomal Mb*cas12a* or codon-modified Lb*cas12a* from inducible promoters and *acr* genes from a plasmid (left). Phage plaque assay with tenfold serial dilutions of phage to assess CRISPR–Cas12a inhibition (right). Phage replication and subsequent host lysis causes clearances in the bacterial lawn. **b**, Western blot on bacterial lysates to assess the effect of Myc-tagged AcrVA2 or control proteins on Cas12a expression. RNAP, RNA polymerase (loading control). **c**, *cas12a* mRNA levels were quantified by qRT–PCR and normalized to *rpoD*. Expression is shown relative to empty vector control using the $^{\Delta\Delta}$Ct method. Points represent technical triplicates ($n = 3$ technical replicates) from one representative experiment; mean ± s.d. is indicated. Experiments were independently repeated at least twice with similar results (**a**–**c**). **d**, Gene expression was quantified as reads per kilobase per million mapped reads (RPKM), normalized to the housekeeping gene *rpoD*, and $\log_2$ transformed. Each point represents one gene. Samples were processed simultaneously and the experiment was not repeated.

abolished AcrVA2 function, restoring Cas12a protein (Fig. 2a–c) and mRNA (Extended Data Fig. 2e) levels. The D89A mutation had a more modest effect, partially reducing AcrVA2 activity.

The inability of AcrVA2 mutants to fully downregulate Cas12a enabled us to test whether these two proteins interact in bacteria. Immunoprecipitation of Myc-tagged AcrVA2 mutants (H286A, R288A and H291A) revealed stable binding to Cas12a (Fig. 2d). These findings indicate that AcrVA2 binds to the Cas12a protein and that binding is not sufficient to inhibit Cas12a activity. Mutation of W79 — a buried residue — also abrogated *cas12a* downregulation but showed no detectable interaction in the pull-down assay, probably due to decreased AcrVA2 stability.

According to a previous report[11], AcrVA2 binds to apo-Cas12a in vitro and co-purifies with a peptide (residues 620–636) near the PAM-interacting domain (PID), but the functional consequences remain unclear. We found that purified maltose-binding protein (MBP)–AcrVA2 did not inhibit DNA cleavage by either pre-assembled Cas12a RNPs (Extended Data Fig. 3a) or apo-Cas12a (Extended Data Fig. 3b), and the MBP tag did not affect AcrVA2 function in vivo (Extended Data Fig. 3c). Furthermore, mutations in AcrVA2 (E98A, D129A and D195A) that disrupt the PID interaction[11] did not prevent *cas12a* downregulation or inhibition in our in vivo assays (Extended Data Fig. 3d,e). These findings reinforce that AcrVA2 binding to Cas12a alone is insufficient to inhibit Cas12a function.

AcrVA2 binds Cas12a N-terminal residues

We next sought to pinpoint the Cas12a sequence sufficient for AcrVA2 binding and subsequent mRNA clearance by generating a series of MbCas12a C-terminal truncations fused to RFP. A minimal fusion containing just the first 30 amino acids of MbCas12a (Cas12a(30 aa)–RFP) was partially downregulated by AcrVA2 (Extended Data Fig. 4a) and co-immunoprecipitated with the inactive AcrVA2(H286A) mutant (Fig. 2e), indicating that this short N-terminal region is sufficient for binding. We hypothesized that the length of the chimera could influence the degree of downregulation. Indeed, fusing Cas12a(30 aa) to the N-terminus of larger proteins, Cas9 (1,368 aa) and Cas12f (422 aa), enabled strong and moderate mRNA downregulation, respectively (Fig. 2f and Extended Data Fig. 4b,c). Moreover, longer N-terminal fragments of Cas12a (for example, approximately 100 aa) enabled more robust mRNA downregulation when fused to these targets (Extended Data Fig. 4). Overall, these results demonstrate that the N-terminal polypeptide of Cas12a is sufficient for AcrVA2-mediated downregulation, establishing a new strategy for targeted gene silencing in bacteria.

We next tested whether the N-terminal polypeptide of Cas12a is necessary for downregulation by AcrVA2. We deleted the first 30 aa of MbCas12a (while providing a start codon) and found that *cas12a* mRNA was no longer downregulated (Extended Data Fig. 5a). Comparing the N-terminal amino acid sequences of LbCas12a and MbCas12a revealed a conserved L^{12}SKT^{15} sequence. Mutating L12 in MbCas12a to alanine diminished AcrVA2-induced downregulation, whereas mutating all four of these residues abolished it (Fig. 2g–i and Extended Data Fig. 5b). As seen with codon-modified versions of *cas12a* (Fig. 1b,c and Extended Data Fig. 1c,d), silent mutations at this site had no effect on downregulation, indicating that the amino acid sequence — rather than nucleic acid sequence — of *cas12a* is the recognized substrate (Fig. 2i).

To assess whether wild-type (WT) AcrVA2 or AcrVA2(H286A) binds to MbCas12a(LSKT>AAAA), we used truncated MbCas12a(560 aa)–RFP that encodes L^{12}SKT^{15} but lacks the secondary PID-binding site (amino acids 620–636)[11]. Co-immunoprecipitation experiments revealed that mutating L^{12}SKT^{15}>AAAA in the MbCas12a polypeptide sequence abolished binding to AcrVA2 (Fig. 2j). Structural modelling with AlphaFold3 further supported the Cas12a peptide binding to the N-terminal domain of AcrVA2, which is consistent with AcrVA2 C-terminal residues (for example, H286) being required for initiating mRNA degradation but not substrate binding (Extended Data Fig. 6).

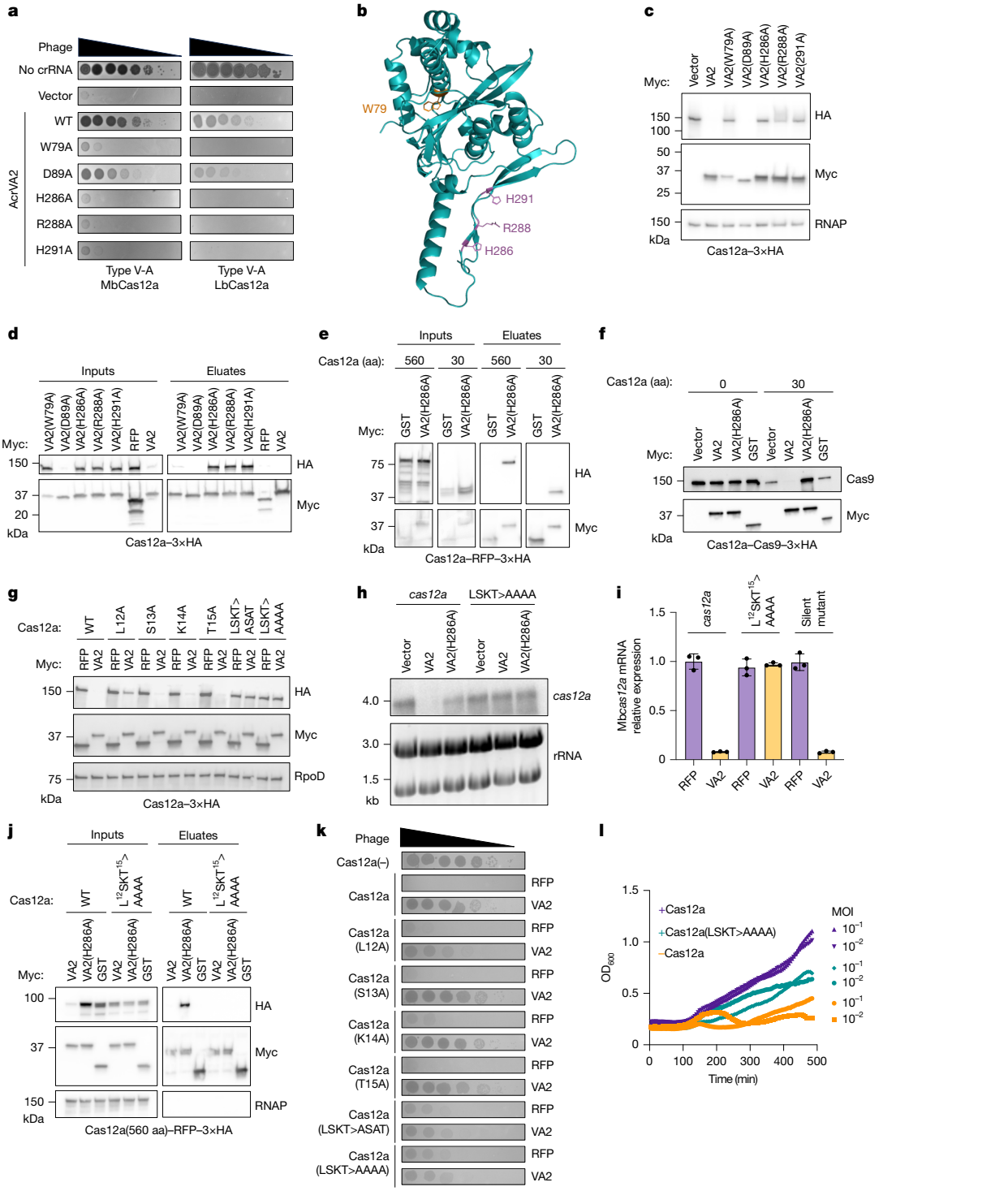


Fig. 2 | AcrVA2 binds to conserved residues near the Cas12a N-terminus to trigger mRNA degradation. a, Plaque assays using tenfold serial dilutions of phage to assess Cas12a-mediated antiphage activity and inhibition by wild-type or mutant AcrVA2. **b**, AlphaFold-predicted structure of AcrVA2 highlighting W79 (orange) and H286, R288 and H291 (purple). The structure has an average local distance difference test score of 87.5. **c**, Western blot analysis of bacterial lysates to assess the effects of Myc-tagged AcrVA2 mutants on Cas12a expression. RNAP served as a loading control. HA, haemagglutinin. **d**, Immunoprecipitation of Myc-tagged wild-type or mutant AcrVA2, or RFP control, from bacterial lysates to assess interaction with Cas12a, followed by SDS–PAGE and western blotting. **e**, Immunoprecipitation of Myc-tagged AcrVA2(H286A) or GST control to assess the interaction with Cas12a–RFP truncation fusions. The numbers indicate the length (amino acids) of Cas12a fragments fused to RFP–3×HA. **f**, Western blot analysis of Cas12a–Cas9 truncation fusions in the presence of AcrVA2–Myc. The numbers indicate the Cas12a fragment length in amino acids. **g**, Western blot showing downregulation of wild-type or mutant Cas12a by AcrVA2–Myc relative to RFP–Myc control. **h**, Northern blot analysis of RNA from bacteria expressing wild-type Cas12a or Cas12a LSKT>AAAA. Ribosomal RNA (rRNA) bands served as loading controls. **i**, *cas12a* mRNA levels quantified by qRT–PCR, normalized to *rpoD*, and expressed relative to empty vector control ($^{\Delta\Delta}$Ct). The points represent technical triplicates ($n = 3$ technical replicates), with mean ± s.d. shown. **j**, Immunoprecipitation assessing interaction between AcrVA2 variants and truncated Cas12a(560 aa)–RFP–3×HA. RNAP was blotted as a loading control. **k**, Plaque assays evaluating inhibition of wild-type or mutant Cas12a by AcrVA2. **l**, Growth curves of phage-infected bacteria expressing MbCas12a variants. Representative experiments are shown; all assays were repeated at least twice with similar results. MOI, multiplicity of infection; OD_{600}, optical density at 600 nm.

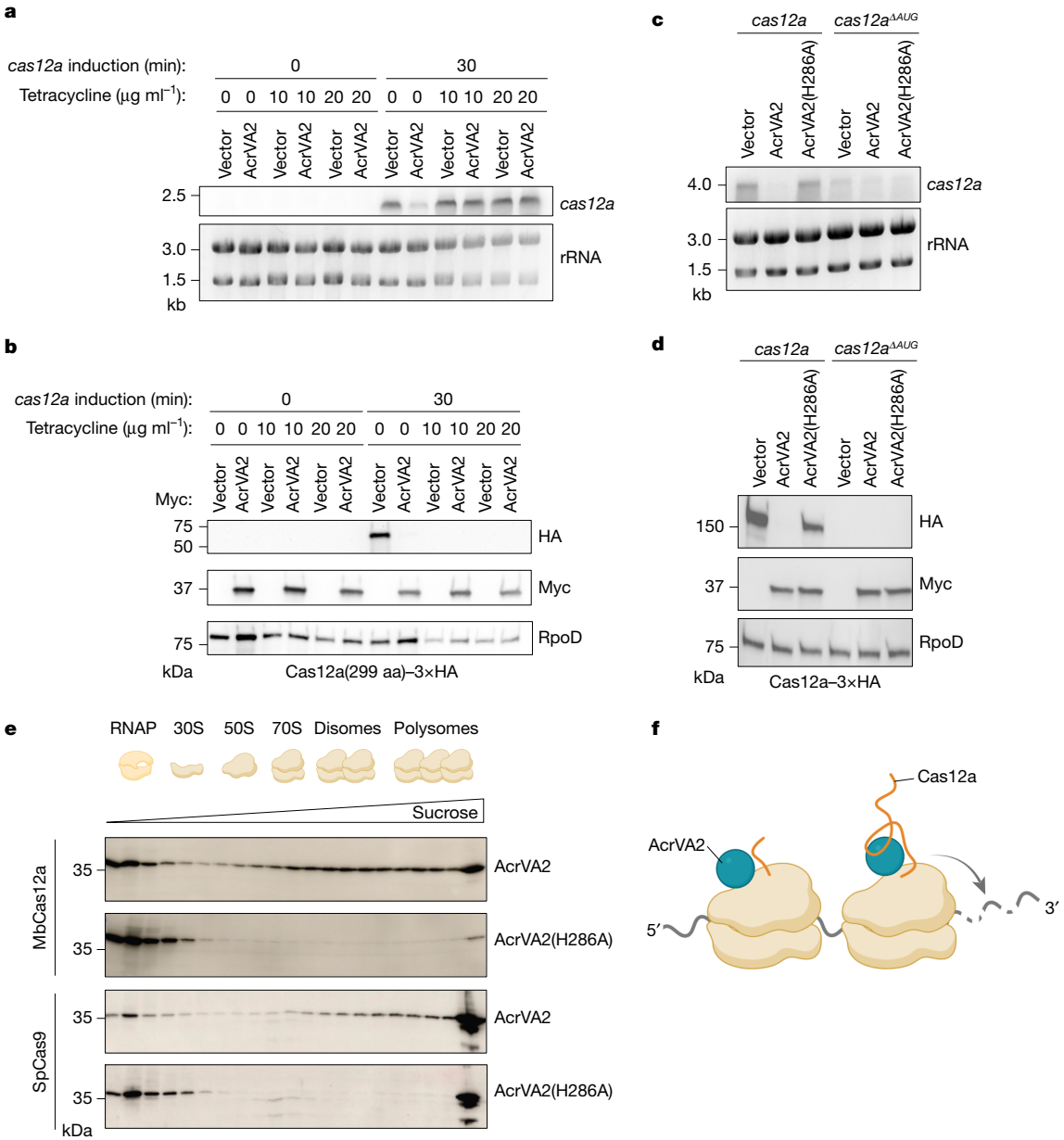


Fig. 3 | *cas12a* mRNA degradation by AcrVA2 requires *cas12a* translation. **a**, Northern blot analysis of Mb*cas12a* mRNA before and after IPTG induction. Time indicates minutes following IPTG addition. Translation was halted by addition of tetracycline at the indicated concentrations. Ribosomal RNA (rRNA) served as a loading control. **b**, Western blot of MbCas12a(299 aa)–3×HA and AcrVA2–Myc from samples corresponding to panel **a**. RpoD was used as a loading control. **c**, Northern blot analysis of Mb*cas12a* transcripts with or without an initiating start codon. rRNA served as a loading control. **d**, Western blot of MbCas12a–3×HA and AcrVA2–Myc from samples corresponding to panel **c**. **e**, Western blot analysis of sucrose gradient fractions from lysates of bacteria co-expressing 3×HA–MbCas12a(299 aa)–SecM and AcrVA2–Myc or control constructs. Fractions corresponding to transcription and translation machinery are indicated. Icons created in BioRender; Marino, N. https://biorender.com/yruipeo (2026). **f**, Model for translation-dependent mRNA degradation: AcrVA2 engages the nascent Cas12a polypeptide during translation, triggering selective degradation of *cas12a* mRNA. Schematic created in BioRender; Marino, N. https://biorender.com/a44txgn (2026). Data were independently repeated at least twice with similar results (**a**–**e**).

We next asked whether the conserved Cas12a amino acids that interact with AcrVA2 are essential for phage defence and anti-CRISPR activity in vivo. These residues lie within the wedge domain and directly contact the crRNA[12]. Mutating L^{12}SKT^{15}>AAAA in Cas12a completely abrogated AcrVA2-mediated inhibition but also caused a thousand-fold reduction in Cas12a antiphage activity (Fig. 2k), presumably due to impaired crRNA binding. Mutating L12 or L^{12}K^{14} similarly diminished both phage targeting and susceptibility to AcrVA2. The decrease in AcrVA2-mediated inhibition correlated closely with reduced Cas12a downregulation across these mutants (Fig. 2g,k and Extended Data Fig. 5b). Phage infection assays in liquid culture corroborated this defect in Cas12a antiphage activity in the absence of AcrVA2 (Fig. 2l). Collectively, these results show that AcrVA2 targets a conserved and functionally important Cas12a N-terminal motif to drive specific mRNA degradation. This mechanism allows AcrVA2 to downregulate diverse Cas12 orthologues while imposing a fitness cost on Cas12a escape mutants.

Translation-dependent mRNA degradation

The simplest explanation for these findings is that AcrVA2 binds to the nascent polypeptide of Cas12a during translation and triggers immediate degradation of *cas12a* mRNA. If so, AcrVA2 should

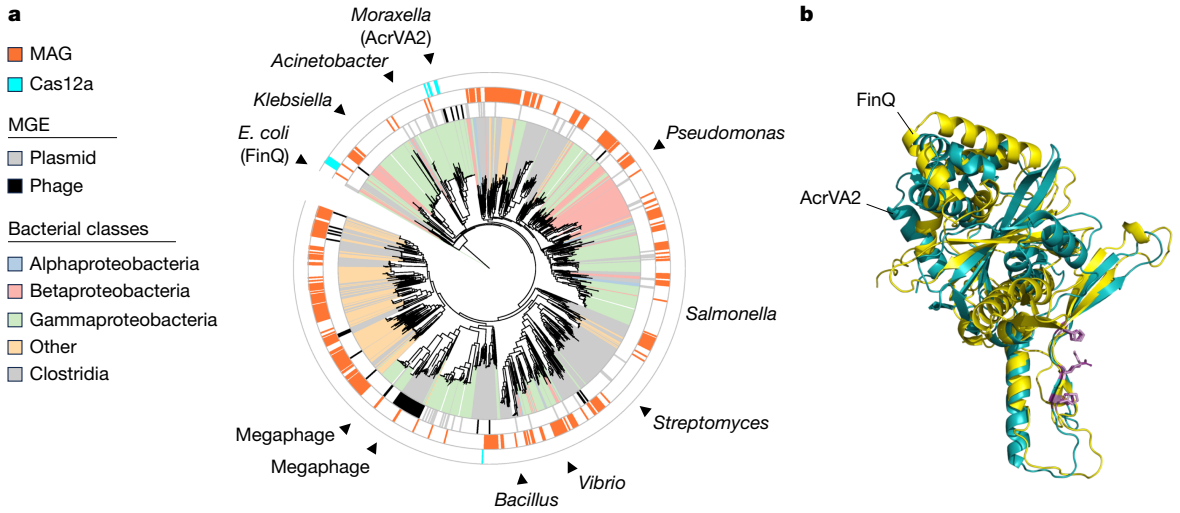


Fig. 4 | AcrVA2 orthologues are encoded on mobile genetic elements across diverse bacteria. a, Approximate maximum likelihood phylogenetic tree of approximately 1,800 AcrVA2 orthologues. The innermost ring indicates bacterial class by colour, whereas the adjacent ring indicates the mobile genetic element (MGE) that the orthologue is present on (where annotated). The middle ring indicates whether the orthologue is found on a metagenomic-assembled genome (MAG), and the outermost ring indicates whether *cas12a* was found in the host genome. The relative branch lengths reflect evolutionary distances between taxa without modification. **b**, Alignment of predicted structures of AcrVA2 (teal) and FinQ (yellow) from AlphaFold using PyMOL. The conserved HRH motif is indicated in light and dark purple for FinQ and AcrVA2, respectively.

only downregulate *cas12a* mRNA when translation is occurring. To test this, we pre-expressed AcrVA2 in cells and then blocked global translation with tetracycline before inducing *cas12a* transcription. This approach enabled *cas12a* transcription but not translation (Fig. 3a,b). Under these conditions, AcrVA2 no longer induced *cas12a* mRNA degradation (Fig. 3a,b). We next asked whether selectively preventing *cas12a* translation by removing its start codon would have a similar effect. As expected, removing the *cas12a* start codon eliminated Cas12a protein expression and decreased *cas12a* mRNA levels, probably due to decreased ribosome occupancy and increased vulnerability to endogenous ribonucleases (Fig. 3c,d). However, AcrVA2 did not further degrade *cas12a* mRNA lacking a start codon, consistent with a translation-dependent mechanism. Overall, these results support a mechanism in which AcrVA2 recognizes Cas12a to initiate targeted co-translational mRNA degradation.

We next asked whether AcrVA2 associates with ribosomes to trigger co-translational clearance of *cas12a* mRNA. To test this, we fractionated bacterial lysates on sucrose gradients and probed for AcrVA2 or AcrVA2(H286A) by immunoblotting. We sought to stabilize Cas12a ribosome-nascent chains by fusing the Cas12a(299 aa) truncation to the SecM arrest peptide, which temporarily stalls ribosomes[13]. AcrVA2, but not inactive AcrVA2(H286A), co-sedimented with ribosomes, disomes and polysomes, consistent with a co-translational mechanism[14] (Fig. 3e and Extended Data Fig. 7a). Of note, AcrVA2 showed a similar sedimentation profile in control strains expressing SpCas9–SecM or MbCas12a(LSKT>AAAA)–SecM (Extended Data Fig. 7b,c). This suggests that AcrVA2 broadly associates with bacterial ribosomes via its C-terminal domain but only triggers mRNA degradation upon binding to specific amino acids in the Cas12a nascent polypeptide (Fig. 3f).

The mechanism by which AcrVA2 triggers *cas12a* mRNA destruction remains mysterious, but in vitro experiments offer some clues. Purified AcrVA2 protein failed to degrade *cas12a* mRNA directly, even in the presence of Cas12a protein provided in *trans* (Extended Data Fig. 8a). Likewise, AcrVA2 had no effect on Cas12a expression when added to, or co-expressed in, the PURE transcription–translation system, which contains only the minimal components for gene expression[15] (Extended Data Fig. 8b,c). These results suggest that AcrVA2 requires additional cellular factors to induce mRNA degradation.

To test whether RNase E, an endoribonuclease involved in global mRNA decay[16], is required, we co-expressed the phage protein Dip (a degradasome inhibitor protein from *P. aeruginosa* phage PhiKZ). Dip inhibited RNase E function, as indicated by growth defects and altered expression of RNase E targets (for example, *pqsB*)[17]. However, RNase E inhibition had no effect on AcrVA2-mediated *cas12a* mRNA degradation (Extended Data Fig. 9), possibly due to redundant mRNA degradation pathways in the cell or the involvement of other factors. We performed immunoprecipitation and mass spectrometry to identify AcrVA2 interactors. Our results confirmed Cas12a as the primary interactor for AcrVA2(H286A) but did not reveal any factors enriched for AcrVA2 relative to AcrVA2(H286A). One possible explanation is that AcrVA2 recruits degradation factors only upon binding the nascent Cas12a polypeptide. As only a small fraction of ribosomes are actively translating Cas12a at any given time, these interactions may be too transient or rare to detect above background using this approach.

AcrVA2 orthologues are broadly distributed on diverse mobile genetic elements

Phylogenetic analysis revealed that AcrVA2 is widespread across diverse bacterial classes, often in species that lack Cas12a (Fig. 4a). We found AcrVA2 homologues encoded on various mobile genetic elements, including plasmids and megaphages. Phage plaque assays showed that many of these homologues do not inhibit MbCas12a or LbCas12a, suggesting that they have different activities or targets (Extended Data Fig. 10). Of note, one homologue, FinQ, was previously identified on I-like plasmids in *Escherichia coli*, where it has been shown to inhibit F-plasmid conjugation[18–20]. Although its mechanism remains unclear, FinQ decreased mRNA levels of F-plasmid transfer genes[20], suggesting a similar mode of action to AcrVA2. The predicted structures of AcrVA2 and FinQ show notable similarities in the C-terminal domain (Fig. 4b), with a root mean square deviation of 1.65 Å across residues 271–347 of FinQ and 245–317 of AcrVA2. These findings suggest that this regulatory mechanism may be broadly used by mobile genetic elements to target diverse systems and facilitate molecular conflict in bacteria.

Discussion

In this study, we have demonstrated that AcrVA2 interrupts Cas12a biogenesis by binding conserved residues near the N-terminus of Cas12a and triggering co-translational mRNA degradation. Several lines of evidence support this mechanism. First, AcrVA2 downregulates mRNA from diverse *cas12a* homologues independently of the promoter or codon usage. Second, the N-terminal region of Cas12a interacts with AcrVA2 and is both necessary and sufficient for downregulation. Third, AcrVA2 co-sediments with actively translating ribosomes independently of Cas12a. Finally, mutations that alter the Cas12a amino acid sequence (but not synonymous mutations) abolish AcrVA2 binding, downregulation and inhibition. Together, these findings support a model in which AcrVA2 broadly associates with translating ribosomes and triggers targeted co-translational mRNA degradation upon binding the Cas12a polypeptide. Consistent with this, AcrVA2 degrades *cas12a* mRNA only when *cas12a* is actively translated into protein. This surprising strategy enables AcrVA2 to recognize conserved and functionally important amino acids in Cas12a and destroy it before it is fully expressed. By targeting the Cas12a polypeptide, rather than the transcript or promoter, AcrVA2 broadly inhibits Cas12a orthologues while also imposing a fitness cost on escape mutations.

Inhibiting Cas12a biogenesis is unlikely to affect pre-existing protein already present in the cell. In our experiments, Cas12a and AcrVA2 were induced simultaneously. Of note, the *M. bovoculi* prophage that encodes AcrVA2 also carries AcrVA1, which inactivates crRNA-loaded Cas12a complexes. Together, these anti-CRISPRs provide dual inhibitory strategies: AcrVA1 inactivates pre-existing Cas12a complexes, whereas AcrVA2 suppresses Cas12a expression. This combined mechanism probably improves phage success during initial infection and stabilizes lysogeny. Similar dual strategies have been observed for anti-CRISPR proteins targeting Cas9, where one protein inactivates the complex, whereas another reduces Cas9 expression, albeit by a different mechanism[21,22].

Some ribonucleases bind to the ribosomal aminoacyl-tRNA site and non-specifically cleave mRNAs during stress[23–25]. In addition, the nascent DnaA polypeptide has been shown to modulate translation elongation in response to nutrient availability[26]. To our knowledge, AcrVA2 is the first example in prokaryotes of a protein that triggers targeted mRNA degradation by recognizing a specific polypeptide sequence. A comparable mechanism exists in eukaryotes: the protein TTC5 binds to the emerging tubulin peptide and recruits SCAPER and the CCR4–NOT complex to degrade the mRNA encoding tubulin[27,28]. Our findings suggest that AcrVA2 uses a similar mechanism to interrupt Cas12a biogenesis, either by recruiting a complex that directly degrades *cas12a* mRNA or by stalling translation, thereby promoting mRNA degradation by cellular ribonucleases.

The arms race between bacteria and phage has yielded many exciting tools and biological discoveries. Here we uncovered a novel strategy for molecular conflict and gene regulation in prokaryotes. This mechanism offers a new paradigm for targeted gene knockdown, with potential applications in bacteria and beyond. For example, its ability to target conserved protein features while limiting escape mutations makes it a promising strategy for future antivirals. The genetic conflict between microorganisms and mobile genetic elements will continue to yield many new insights and tools in the years to come.

Online content

Any methods, additional references, Nature Portfolio reporting summaries, source data, extended data, supplementary information, acknowledgements, peer review information; details of author contributions and competing interests; and statements of data and code availability are available at https://doi.org/10.1038/s41586-026-10440-8.

1. Murtazalieva, K., Mu, A., Petrovskaya, A. & Finn, R. D. The growing repertoire of phage anti-defence systems. *Trends Microbiol.* **32**, 1212–1228 (2024).
2. Mayo-Muñoz, D., Pinilla-Redondo, R., Camara-Wilpert, S., Birkholz, N. & Fineran, P. C. Inhibitors of bacterial immune systems: discovery, mechanisms and applications. *Nat. Rev. Genet.* **25**, 237–254 (2024).
3. Davidson, A. R. et al. Anti-CRISPRs: protein inhibitors of CRISPR-Cas systems. *Annu. Rev. Biochem.* **89**, 309–332 (2020).
4. Marino, N. D. Phage against the machine: discovery and mechanism of type V anti-CRISPRs. *J. Mol. Biol.* **435**, 168054 (2023).
5. Knott, G. J. et al. Broad-spectrum enzymatic inhibition of CRISPR-Cas12a. *Nat. Struct. Mol. Biol.* **26**, 315–321 (2019).
6. Zhang, H. et al. Structural basis for the inhibition of CRISPR-Cas12a by anti-CRISPR proteins. *Cell Host Microbe* **25**, 815–826.e4 (2019).
7. Marino, N. D. et al. Discovery of widespread type I and type V CRISPR-Cas inhibitors. *Science* **362**, 240–242 (2018).
8. Varadi, M. et al. AlphaFold Protein Structure Database: massively expanding the structural coverage of protein-sequence space with high-accuracy models. *Nucleic Acids Res.* **50**, D439–D444 (2022).
9. Varadi, M. et al. AlphaFold Protein Structure Database in 2024: providing structure coverage for over 214 million protein sequences. *Nucleic Acids Res.* **52**, D368–D375 (2024).
10. Abramson, J. et al. Accurate structure prediction of biomolecular interactions with AlphaFold 3. *Nature* **630**, 493–500 (2024).
11. Peng, C. et al. Structural study on anti-CRISPR protein AcrVA2. *Prog. Biochem. Biophys.* **48**, 77–87 (2021).
12. Swarts, D. C., van der Oost, J. & Jinek, M. Structural basis for guide RNA processing and seed-dependent DNA targeting by CRISPR-Cas12a. *Mol. Cell* **66**, 221–233.e4 (2017).
13. Gersteuer, F. et al. The SecM arrest peptide traps a pre-peptide bond formation state of the ribosome. *Nat. Commun.* **15**, 2431 (2024).
14. Gerovac, M. et al. Phage proteins target and co-opt host ribosomes immediately upon infection. *Nat. Microbiol.* **9**, 787–800 (2024).
15. Shimizu, Y. et al. Cell-free translation reconstituted with purified components. *Nat. Biotechnol.* **19**, 751–755 (2001).
16. Mackie, G. A. RNase E: at the interface of bacterial RNA processing and decay. *Nat. Rev. Microbiol.* **11**, 45–57 (2013).
17. Geslain, S. A. M. et al. Critical functions and key interactions mediated by the RNase E scaffolding domain in *Pseudomonas aeruginosa*. *PLoS Genet.* **21**, e1011618 (2025).
18. Gasson, M. & Willetts, N. Transfer gene expression during fertility inhibition of the *Escherichia coli* K12 sex factor F by the I-like plasmid R62. *Mol. Gen. Genet.* **149**, 329–333 (1976).
19. Gasson, M. J. & Willetts, N. S. Further characterization of the F fertility inhibition systems of "unusual" Fin+ plasmids. *J. Bacteriol.* **131**, 413–420 (1977).
20. Gaffney, D., Skurray, R. & Willetts, N. Regulation of the F conjugation genes studied by hybridization and tra-lacZ fusion. *J. Mol. Biol.* **168**, 103–122 (1983).
21. Osuna, B. A. et al. *Listeria* phages induce Cas9 degradation to protect lysogenic genomes. *Cell Host Microbe* **28**, 31–40.e9 (2020).
22. Osuna, B. A. et al. Critical anti-CRISPR locus repression by a bi-functional Cas9 inhibitor. *Cell Host Microbe* **28**, 23–30.e5 (2020).
23. Leroy, M. et al. Rae1/YacP, a new endoribonuclease involved in ribosome-dependent mRNA decay in *Bacillus subtilis*. *EMBO J.* **36**, 1167–1181 (2017).
24. Goeders, N., Drèze, P.-L. & Van Melderen, L. Relaxed cleavage specificity within the RelE toxin family. *J. Bacteriol.* **195**, 2541–2549 (2013).
25. Lalaouna, D. & Massé, E. Cut in translation: ribosome-dependent mRNA decay. *EMBO J.* **36**, 1120–1122 (2017).
26. Felletti, M., Romilly, C., Wagner, E. G. H. & Jonas, K. A nascent polypeptide sequence modulates DnaA translation elongation in response to nutrient availability. *eLife* **10**, e71611 (2021).
27. Lin, Z. et al. TTC5 mediates autoregulation of tubulin via mRNA degradation. *Science* **367**, 100–104 (2020).
28. Höpfler, M. et al. Mechanism of ribosome-associated mRNA degradation during tubulin autoregulation. *Mol. Cell* **83**, 2290–2302.e13 (2023).

Publisher's note Springer Nature remains neutral with regard to jurisdictional claims in published maps and institutional affiliations.

Springer Nature or its licensor (e.g. a society or other partner) holds exclusive rights to this article under a publishing agreement with the author(s) or other rightsholder(s); author self-archiving of the accepted manuscript version of this article is solely governed by the terms of such publishing agreement and applicable law.

© The Author(s), under exclusive licence to Springer Nature Limited 2026

Methods

Bacterial strains and growth conditions

The *P. aeruginosa* strain PAO1 and *E. coli* strains MG1655 and BW25113 were used in this study (Supplementary Table 1). PAO1 was grown at 37 °C in lysogeny broth (LB) or on LB agar, which was supplemented with 50 μg ml^{-1} gentamicin, 30 μg ml^{-1} tetracycline or 200 μg ml^{-1} carbenicillin (as needed for plasmid selection) or with 30 μg ml^{-1} gentamicin or 100 μg ml^{-1} carbenicillin (for plasmid maintenance). MG1655 and BW25113 were grown at 37 °C on LB agar or in medium, which was supplemented with 10 μg ml^{-1} gentamicin or 100 μg ml^{-1} carbenicillin (for plasmid selection and maintenance). Strains were grown to saturation and frozen in 15% glycerol at −80 °C for long-term storage.

Bacterial colonies used for experiments were randomly chosen from an agar plate and grown overnight at 37 °C while shaking at 200 rpm. Saturated cultures were diluted 1:100 into LB supplemented with antibiotics and inducers and then grown to OD_{600} of approximately 0.4–1. Genes regulated by the *tac* promoter or *lac* operator were induced with 1 mM isopropyl β-D-1-thiogalactopyranoside (IPTG). Genes expressed from the *pBAD* promoter were induced with 0.3% arabinose unless otherwise indicated. The volumes of bacterial cultures were normalized and harvested by centrifugation at 8,000*g* for 2 min (1–2 ml cultures) or 10 min (5–10 ml cultures).

Cloning

Native Mb*cas12a* genes were amplified from genomic DNA of *M. bovoculi* strain 237 or from plasmids pKEW336-MbCas12a or pKEW106-MbCas12a-58069 and cloned into linearized pTN7C130 using HiFi assembly[5,29]. The pTN7C130 vector (a gift from J. Peters) is a mini-Tn7 vector that integrates into the attTn7 site of *P. aeruginosa* and expresses cargo genes from the *pBAD* promoter. MbCas12a mutants were generated from the original vector (pTN7C130-huMbCas12a, which expresses human-codon-optimized MbCas12a and a C-terminal 3×HA tag) using site-directed mutagenesis. Specifically, HA-tagged constructs were generated using round-the-world PCR with non-overlapping primers encoding the desired mutations. These primers were phosphorylated using T4 polynucleotide kinase (NEB) before PCR, and the resulting amplicons were digested with DpnI for 1–2 h at 37 °C to destroy the template. The products were ligated using T4 ligase (NEB) at room temperature for 1 h or overnight at 16 °C. pTN7C130-Cas12a(ΔAUG) and pTN7C130-Cas12a(Δ1–30 aa) were generated from the pTN7C130-MbCas12a vector using round-the-world PCR and ligation, as described above. Primers were designed to omit the start codon (pTN7C130-Cas12a(ΔAUG)) or the first 30 aa (pTN7C130-Cas12a(Δ1–30 aa)) with an added start codon. Cas12a C-terminal truncations were generated by amplifying the desired sequence from the pTN7C130-MbCas12a vector and fusing the resulting fragment to sequences encoding mRFP or SecM via HiFi assembly (NEB).

pTN7C185-Cas12a-Cas9-3×HA vectors were generated by amplifying truncated fragments of Cas12a from pTN7C130-MbCas12a and full-length SpCas9 from pTN7C130.1 (a gift from J. Peters) and assembling them together into linearized pTN7C185 via HiFi assembly. pTN7C185-Cas12a-Cas12f-3×HA was generated using a similar method, but the gene encoding AsCas12f was amplified from pET47b-T7-AsCas12f-WT (Addgene).

Anti-CRISPR (AcrIIA4, AcrVA1, AcrVA2 and AcrVA2.1) and control genes (RFP and GST) encoding a C-terminal Myc tag were cloned near the NcoI and HindIII sites of pHERD20T-Myc and pHERD30T-Myc using Gibson Assembly (NEB) or HiFi assembly (NEB). Backbone vectors were generated by digestion at the NcoI and HindIII sites or by round-the-world PCR. Anti-CRISPR genes and control genes were amplified (along with the *pBAD* promoter and *araC* gene) from pHERD30T-based or pHERD20T-based constructs and ligated into the SacI and HindIII sites of CTX2-mini[30].

Bacterial transformations for cloning were performed using *E. coli* DH5α (NEB) or XL-1 blues (QB3 MacroLab) according to the manufacturer's instructions. Plasmids were miniprepped from the resulting colonies (Zymo) and sequenced via Sanger and whole-plasmid sequencing. Plasmids and plasmid sequences are available on request.

Strain engineering

Transformations of the *P. aeruginosa* PAO1 strain were performed using standard electroporation protocols. In brief, 1 ml of overnight culture was washed twice in 300 mM sucrose or 10% glycerol and concentrated tenfold. The resulting competent cells were transformed with 30 ng or 300 ng plasmid (for extrachromosomal uptake or chromosomal integration, respectively), incubated in antibiotic-free LB for 1 h at 37 °C, plated on LB agar with selective media and grown overnight at 37 °C. Chromosomal integration of pTN7C130 or pTN7C185 derivatives via Tn7 transposition was achieved by co-electroporation with pTNS3, as previously described[31,32].

Chromosomal integration of pTN7C130 or pTN7C185 derivatives into *E. coli* strain MG1655 was achieved by conjugation, as previously described[33]. In brief, WM6026 donor strains that are auxotrophic for diaminopimelic acid (DAP) were made chemically competent using standard protocols[34]. These competent cells were transformed with pTN7C130 or pTN7C185 derivatives or Tn7 helper plasmid by heat shock transformation with selection on LB agar plates supplemented with 30 μg ml^{-1} gentamicin and 300 μM DAP overnight at 37 °C. Both the TN7 plasmid and helper plasmid were delivered to *E. coli* MG1655 via triparental mating and grown overnight at 37 °C on LB supplemented with 300 μM DAP. The resulting bacterial lawns were scraped, diluted and plated on LB agar supplemented with 10 μg ml^{-1} gentamicin to select for MG1655 that stably integrated the pTN7 vector (and select against the DAP-dependent WM6026 donors). Integration at the Tn7 locus of MG1655 was confirmed by PCR and Sanger sequencing. *E. coli* strains were made chemically competent using established protocols and were transformed with pHERD20T or pHERD30T derivatives via heat shock transformation[34].

Phage isolation and storage

Phage lysates were generated by mixing 10 μl phage lysate with 150 μl overnight culture of PAO1 and 4 ml of molten 0.7% top agar, plating the mixture on 1% LB agar, and growing plates overnight at 30 °C. The phage plaques were harvested by adding 3 ml SM buffer (100 mM NaCl, 8 mM $MgSO_4$, 50 mM Tris-HCl, pH 7.5, and 0.01% gelatin) to the plate and incubating at room temperature for 10 min. Approximately 1.5 ml supernatant was collected and transferred to a fresh tube containing 80 μl chloroform. The supernatant was mixed with the chloroform by gentle rocking at room temperature for 10 min. The supernatant was then centrifuged at full speed for 5 min to pellet bacteria, and the resulting supernatant was transferred to a fresh tube treated containing 40 μl chloroform. Phage lysates were stored at 4 °C.

Bacteriophage plaque assays

Plaque assays were performed using 1% LB agar plates and 0.7% LB top agar, both of which were supplemented with 10 mM $MgSO_4$. Overnight culture (150 μl) was resuspended in 3–4 ml molten top agar and plated on LB agar to create a bacterial lawn. Tenfold serial dilutions of phage were prepared in SM phage buffer (100 mM NaCl, 8 mM $MgSO_4$, 50 mM Tris-HCl, pH 7.5, and 0.01% gelatin), spotted onto the plate and incubated overnight at 30 °C. Agar plates were supplemented with 1 mM IPTG and 0.3% arabinose for assays performed with LbCas12a-expressing strains and 0.3% arabinose for assays performed with MbCas12a-expressing strains. Agar plates were supplemented with 30 μg ml^{-1} gentamicin or 100 μg ml^{-1} carbenicillin for pHERD30T and pHERD20T retention, respectively. Anti-CRISPR activity was assessed by measuring replication of the CRISPR-sensitive phage JBD30 on bacterial lawns relative to the vector control. Plate images were obtained

using the Gel Doc EZ Gel Documentation System (Bio-Rad) and Image Lab (Bio-Rad) software.

Growth assays

Overnight cultures of *P. aeruginosa* encoding wild-type MbCas12a, MbCas12a(LSKT>AAAA) or no MbCas12a were diluted 1:100 in LB supplemented with 10 mM $MgSO_4$ and 0.3% arabinose. Of diluted bacteria, 90 µl was added to a 96-well plate and then infected with 10 µl $DMS3_{vir}$ phage diluted tenfold in SM phage buffer. These infections proceeded for 24 h in a Synergy H1 microplate reader with continuous, double orbital shaking at 37 °C. Measurements at OD_{600} were taken every 5 min. Dilutions of bacteria and phage were plated to determine the number of colony-forming units (CFUs) and plaque-forming units (PFUs), respectively. The multiplicity of infection was determined by dividing the number of PFUs by CFUs.

Overnight cultures of *E. coli* encoding MbCas12a and pHERD20T or pHERD20T-Dip were diluted 1:100 in LB supplemented with 1% arabinose. Of diluted bacteria, 100 µl was added to each well of a 96-well plate and grown for 16 h in a Tecan microplate reader with continuous, double orbital shaking at 37 °C. Measurements at OD_{600} were taken every 5 min.

Immunoprecipitations

PAO1 strains were grown overnight at 37 °C in LB supplemented with appropriate antibiotics for plasmid retention. Induction media (50 ml per strain) were inoculated 1:100 with overnight culture and grown at 37 °C until OD_{600} of 0.5–1. Samples were normalized by optical density and harvested at 8,000*g* for 10 min. Pellets were stored at −80 °C or immediately resuspended in 1 ml lysis buffer (50 mM Tris, pH 7.5, 250 mM NaCl, 20 mM $MgCl_2$, 5% glycerol and 1% NP-40) supplemented with 0.25 mg ml^{-1} lysozyme and mini protease inhibitor cocktail (Roche). Samples were left on ice for 30 min, then sonicated twice for 10 s at 30% amplitude at 4 °C (QSonica). Debris was spun down at 14,000 rpm for 10 min at 4 °C and supernatants were collected. One-tenth of the sample volume was retained for input analysis, and the remaining volume was rotated overnight at 4 °C with 45 µl of anti-Myc magnetic beads from Cell Signaling Technology (5698) or Pierce (88843) to enrich for Myc-tagged constructs. For western blot or silver stain analysis, beads were washed 4 ×5 min while rotating using 1 ml wash buffer (50 mM Tris, 250 mM NaCl, 20 mM $MgCl_2$, 5% glycerol and 0.1% NP-40) per wash. Eluates were boiled off from the beads in 50 µl of Laemmli buffer (Bio-Rad). For mass spectrometry analysis, beads were washed 3 ×5 min with the same wash buffer before a final 5-min wash with buffer lacking NP-40 and glycerol. The beads were then frozen at −80 °C until processing for mass spectrometry.

Western blots

PAO1 strains were grown overnight at 37 °C in LB supplemented with appropriate antibiotics for plasmid retention. Induction media (8 ml per strain) were inoculated 1:100 with overnight culture and grown at 37 °C until OD_{600} of 0.5–1. Samples were normalized by optical density and harvested at 8,000*g* for 2 min. Pellets were stored at −80 °C or immediately resuspended in 1 ml lysis buffer (50 mM Tris, pH 7.5, 250 mM NaCl, 20 mM $MgCl_2$, 5% glycerol and 1% NP-40) supplemented with 0.25 mg ml^{-1} lysozyme and mini protease inhibitor cocktail (Roche). Samples were left on ice for 30 min, then sonicated twice for 10 s at 20% amplitude at 4 °C (QSonica). Debris was spun down at 14,000 rpm for 10 min at 4 °C and supernatants were collected.

Samples (from immunoprecipitation or lysate preparation) were boiled for 10 min in Laemmli buffer supplemented with BME, separated by SDS–PAGE, and transferred to polyvinylidene difluoride membranes. Membranes were blocked in blocking buffer (5% milk in TBS supplemented with 2.5% Tween-20) for 1 h at room temperature and then incubated overnight at 4 °C with primary antibody in blocking buffer. Cas12a–HA was detected using horseradish peroxidase (HRP)-conjugated HA antibody (Roche) at 1:5,000 dilution. LbCas12a was detected using LbCpf1 (strain ND2006) mouse monoclonal antibody (91982S, Cell Signaling Technology) at 1:2,000 dilution. Myc-tagged proteins were detected using Myc-tag (9B11) mouse monoclonal antibody (2276S, Cell Signaling Technology) at 1:5,000 dilution. RNAP was detected using anti-*E. coli* RNA polymerase-β (663905, BioLegend) at 1:5,000 dilution. Goat anti-mouse IgG secondary antibody conjugated to HRP (62-6520, Invitrogen) was used for anti-Myc, anti-LbCpf1 and anti-RNAP primary antibodies. HRP was detected using enhanced chemiluminescence (ECL) kit (Pierce). Membranes were stripped between blots by incubation in stripping buffer (Thermo Fisher) for 10–15 min then washed 2 ×5 min with PBS or TBST.

Mass spectrometry

Immunoprecipitated proteins were denatured by the addition of 1.7 M urea, 50 mM Tris (pH 8) and 1 mM dithiothreitol for 15 min at 60 °C. After cooling to room temperature, cysteines were reduced and alkylated by the addition of 10 mM tris(2-carboxyethyl)phosphine and 40 mM 2-chloroacetamide. The lysates were then incubated at 45 °C for 5 min with shaking at 1,500 rpm. Finally, 1 µg of trypsin (Promega) was added to the lysate, and proteolytic digestion was performed overnight at 37 °C. The next day, the resulting peptides were acidified to a pH of approximately 2 and desalted in micro-C18 tips (Nest Group). The desalted eluates were dried by vacuum centrifugation and resuspended in 20 µl of 0.1% formic acid before injection of 2 µl for mass spectrometry analysis on a Thermo Scientific Oribtrap Fusion mass spectrometer using data-dependent acquisition. The resulting data were searched using MaxQuant (v1.6.12.0)[35] using default settings and against both the *P. aeruginosa* protein sequences (Uniprot) supplemented with the AcrVA2, AcrVA2.1 and AcrVA2(H286A) sequences. The resulting proteins (filtered to a 1% false discovery rate) were analysed to determine high-confidence protein–protein interactions by SAINTexpress[36] and filtered to a 5% false discovery rate.

Protein purification

The plasmids used for MbCas12a(33362) and AcrVA1 protein purification were previously published and encode the following, in order from the N-terminus: a 10× His tag, MBP, TEV protease cleavage site, the Cas12a sequence and a C-terminal NLS sequence for gene-editing assays[5,29]. Anti-CRISPR plasmids for AcrVA2, AcrVA2(H286A) and AcrIIA4 protein purification were generated by amplifying the backbone from the AcrVA1 plasmid and cloning in other open reading frames using HiFi assembly (NEB). *E. coli* Rosetta2 cells freshly transformed with each plasmid were grown overnight in LB and subcultured in LB until OD_{600} of approximately 0.5. Cells were induced with 0.4 mM IPTG and grown overnight at 16–20 °C. Cells were harvested and resuspended in lysis buffer (20 mM Tris-HCl, pH 8, at 4 °C, 150 mM NaCl, 10 mM imidazole, 0.5% Triton X-100, 10% glycerol, 1 mM TCEP or dithiothreitol supplemented with mini complete EDTA-free protease inhibitor (Roche) and 1 mM phenylmethylsulfonyl fluoride (PMSF)), lysed by sonication and purified using Ni-NTA resin. The eluted proteins were cleaved with TEV protease overnight at 4 °C (except for AcrVA2, which precipitated out of solution upon cleavage), and purified by size-exclusion chromatography using the following buffer (20 mM HEPES, pH 7.5, 150 mM KCl, 20 mM $MgCl_2$, 10% glycerol and 1 mM dithiothreitol).

In vitro DNA cleavage assays

Cas12a cleavage assays were performed using purified, TEV-cleaved MbCas12a(33362) protein and crRNAs that were synthesized commercially (IDT). Double-stranded DNA templates were amplified from plasmids and purified using DNA Clean and Concentrator Kit (Zymo). Purified 10×His–MBP–AcrVA2 or control protein was incubated with Cas12a RNP complexes that were formed as follows: crRNA was diluted to 300 nM in water, heated at 70 °C for 5 min, then allowed to cool down to room temperature. crRNA was mixed with 1 µM Cas12a protein

for a final concentration of 30 nM in NEBuffer r2.1 reaction buffer. The reaction was incubated at 37 °C for 10 min. Purified Acr or control protein was diluted separately in the reaction buffer and added to the reaction at a 1:1 or 10:1 concentration relative to Cas12a RNPs. Pre-formed RNPs and Acr proteins were incubated at 37 °C for 30 min before template DNA was added. Cleavage reactions were allowed to go on for 30 min up to 2 h at 37 °C. The reactions were halted by incubating with proteinase K for 10 min at room temperature. Alternatively, purified MBP–AcrVA2 or control protein was incubated with apo-Cas12a for 30 min at room temperature before the addition of crRNA and template DNA. Once crRNA and template DNA were added, reactions were incubated at 37 °C for 30 min up to 2 h before the addition of proteinase K. Reactions were loaded onto 1% TAE agarose gels and resolved by electrophoresis. Gels were post-stained with SYBR Gold (Invitrogen) for 1 h at room temperature and imaged using Bio-Rad Gel Doc EZ Imager.

In vitro RNA cleavage assays

In vitro RNA cleavage assays were performed by incubating purified 10×His–MBP–AcrVA2 or control protein with Cas12a or SpyCas9 mRNA ± purified MbCas12a(33362). The first 300 nucleotides of *cas12a* and *cas9* mRNA were transcribed from a DNA template at 37 °C for 16 h using the HiScribe T7 Quick In Vitro Transcription Kit (NEB). The resulting RNA was treated with DNase and purified with the miRNeasy kit (Qiagen). *cas12a* or *cas9* mRNA was added to cleavage reactions with 30 nM anti-CRISPR protein ± 30 nM MbCas12a(33362) protein in cleavage buffer (20 mM HEPES-HCl, pH 7.5, 150 mM KCl, 10 mM $MgCl_2$ and 0.5 mM TCEP). Reactions were incubated at 37 °C for 1 h and were then heated with RNA dye at 70 °C for 10 min to stop the reaction. The reaction products were resolved in TBE–urea gels by electrophoresis and stained with SYBR Gold.

Transcription–translation assays

In vitro transcription–translation assays were performed using the PURE NEBExpress system (NEB). MbCas12a(560 aa)–RFP–3×HA was expressed from approximately 150 ng of DNA template for 2 h at 37 °C in reactions supplemented with 1 μM MBP or MBP–AcrVA2 protein. Alternatively, MbCas12a(560 aa)–RFP–3×HA was incubated with equimolar DNA templates expressing AcrVA2–Myc or GST–Myc. Reaction products were assessed by SDS–PAGE and western blot.

RNA extraction and qRT–PCR

Induction media (8 ml per strain) were inoculated 1:100 with overnight cultures and allowed to grow to OD_{600} of 0.5–1. Bacteria were harvested and resuspended in 800 μl water and mixed 1:1 with pre-heated lysis buffer, which consisted of 100 μl of 8× lysis solution (0.3 M sodium acetate, 8% sodium dodecyl sulfate and 16 mM EDTA) mixed with 700 μl acid phenol–chloroform per sample and heated at 65 °C for 15 min. The lysate was then incubated at 65 °C for 5–10 min with frequent vortexing. Samples were spun at 12,000*g* for 15 min at 4 °C and the upper aqueous layer was collected. Samples were extracted two times with equivalent volumes of chloroform and incubated overnight at −20 °C with three volumes of 100% ethanol. Samples were harvested at 14,000 rpm for 15 min at 4 °C and washed with 75% ethanol. Pellets were resuspended in Milli-Q water and assessed for yield and purity using a spectrophotometer.

Purified RNA was treated for contaminating DNA using the Turbo DNase kit (Invitrogen). Relative mRNA levels of *cas12a*, *rfp* and *rpoD* control were assessed using the Luna Universal One-Step qRT–PCR kit (NEB) according to the manufacturer's instructions. Primers were assessed for efficiency of amplification and controls lacking reverse transcriptase were used in all experiments. *rpoD* was used as a loading control to normalize expression. Experiments were repeated at least three times (from RNA extraction to qRT–PCR analysis) on randomly chosen colonies (typically from different transformations).

RNA sequencing

RNA was extracted from bacterial strains expressing MbCas12a and either AcrVA1, AcrVA2, AcrVA2.1, AcrVA2(H286A) or AcrIIA4 according to the protocol described above. Purified RNA was treated with Turbo DNase (Invitrogen) for 30 min at 37 °C and then purified by phenol–chloroform extraction. RNA was prepared for sequencing using the SMARTER Stranded RNA sequencing kit (Takara Bio) according to the manufacturer's instructions with the following parameters: fragmentation was performed for 4 min, and PCR amplification of the final library was carried out for ten cycles. Amplified libraries were quantified using a Qubit 4.0 fluorometer (Life Technologies) and sequenced on an Illumina HiSeq in single end format (50 bp) with one 6-bp index read. Sequencing adapters were trimmed from the reads at the 3′ end, and 3 bp were additionally trimmed from the 5′ end of every read to account for the template switching activity of the reverse transcriptase using cutadapt. Trimmed reads were mapped to the PAO1 reference genome and to the Cas12a coding DNA sequence using bowtie2. RPKM values were then calculated per gene and mappings were visualized using IGV.

Gene expression was quantified as RPKM. Within each sample, gene expression was normalized to the housekeeping gene *rpoD* by dividing the RPKM of each gene by the corresponding *rpoD* RPKM value. A pseudocount (0.001) was added before $\log_2$ transformation to prevent undefined values. $\log_2$-Transformed normalized expression values were used for comparative visualization of AcrVA2 and control samples. Scatter plots were generated using GraphPad.

RNA extraction and northern blot

Overnight cultures of bacteria were diluted 1:100 in media (typically 25 ml) supplemented with antibiotics for plasmid retention and with inducers for protein expression. Cultures were grown, shaking, at 37 °C until OD_{600} of 0.4–1.0. Approximately 5–12 ml of culture were normalized and harvested for each sample by centrifugation. Pellets were flash frozen and stored at −80 °C or used immediately for RNA extraction. Pellets were resuspended in 1 ml STE buffer supplemented with 1% SDS and then transferred to a fresh tube with 0.65 ml acid phenol–chloroform preheated to 65 °C. Samples were shaken at 1,400 rpm at 65 °C for 5 min with regular vortexing. Tubes were placed on ice for 5 min and then spun in a microcentrifuge at room temperature for 5 min at maximum speed. The top aqueous layer was harvested and mixed with 0.65 ml acid phenol–chloroform at room temperature. Samples were vortexed and shaken at 1,400 rpm at room temperature for 5 min. Samples were spun in a microcentrifuge for 5 min at maximum speed. The top aqueous layer was harvested and mixed in a fresh tube with 0.65 ml chloroform. The samples were vortexed and spun down at maximum speed for 2 min at room temperature. The aqueous layer was mixed with sodium acetate and precipitated with isopropanol using standard protocols. Pellets were washed with 80% ethanol and resuspended with 50 μl DEPC-treated water.

RNA samples (approximately 5 μg) were resolved by agarose gel electrophoresis and probed by northern blot using the Northern Max kit (Ambion). RNA was transferred from the gel to a nylon membrane using downward transfer (as described in the manufacturer's instructions). The resulting membranes were crosslinked with a 10-mJ ultraviolet burst over 30 s (Stratagene) and either stored at −20 °C or blotted immediately. The membrane was blocked with UltraHyb buffer and hybridized at 68 °C overnight with a radiolabelled *cas12a* mRNA probe. The probe was synthesized from a DNA template using the MAXIscript T7 transcription kit and α-32P-labelled uridine triphosphate immediately before hybridization. After hybridization, the membrane was washed four times (twice with low stringency buffer and twice with high stringency buffer), each for 5 min while rotating at 68 °C. The blots were developed using a phosphor screen and Typhoon imager.

Translation inhibition experiments

MG1655 strains encoding MbCas12a((237)(299 aa))–RFP–3×HA and pHERD20T or pHERD20T-AcrVA2-Myc were grown overnight and diluted 1:100 in LB medium supplemented with 100 μg ml^{-1} carbenicillin and 0.1% arabinose to induce AcrVA2–Myc expression. Bacteria were grown at 37 °C to OD_{600} of approximately 0.5 and divided into three flasks, each treated with 0, 10 or 20 μg ml^{-1} tetracycline. Cultures were returned to the shaking incubator to grow until they reached OD_{600} of approximately 0.6–0.8. Different volumes of each bacterial culture were harvested by centrifugation to normalize cell count (time = 0, before Cas12a induction). The remaining flask volumes were treated with 1 mM IPTG to induce Cas12a expression for 30 min, and volumes of each bacterial culture were normalized and harvested by centrifugation (time = 30 min). Bacterial pellets were frozen at −80 °C or immediately subjected to RNA extraction.

Gradient fractionation of ribosomes

Cells were grown in 50 ml LB medium at 37 °C at 220 rpm to OD of 0.6. Cas12 and AcrVA2 were induced with 1% arabinose for 10 min. The cells were spun down at 13,500*g* for 4 min and the pellet was flash frozen in liquid nitrogen resulting in approximately 100 μl pellet. Cells were resuspended in 800 μl ice-cold lysis buffer (20 mM Tris-HCl, pH 7.5, 150 mM KCl, 70 mM $MgCl_2$, 1 mM dithiothreitol and 2 mM PMSF) and transferred to the bead-based lysis matrix E (MP Biomedicals), followed by bead beating in the FastPrep-24 5 G (MP Biomedicals) for 45 s at 6.0 m s^{-1}. The lysed cells were cleared at 15,000*g* for 10 min at 4 °C. The lysate was layered on top of a 10–40% sucrose gradient in lysis buffer without PMSF. The gradient was resolved in a SW41 rotor (Beckman Coulter) for 2.5 h at 166,000*g* at 4 °C. The gradient was harvested in 590-μl fractions. Gradient samples were analysed by SDS–PAGE and western blotting. Myc tag was detected with anti-Myc antibody (1:10,000, mouse; M4439, Sigma), HA tag with anti-HA antibody (1:10,000, rabbit; 3724S, Cell Signaling Technology). Antibodies were diluted in 5% BSA in TBST. The following secondary antibodies were used: anti-mouse HRP (1:10,000, goat; ab97040, Abcam) and anti-rabbit HRP (1:10,000, goat; 31460, Thermo Scientific).

Phylogenetic analysis

The sequence of AcrVA2 from *M. bovoculi* 58069 was used to query the NCBI non-redundant protein database with PSI-BLAST (three rounds, default parameters)[37]. Hits were filtered to remove any with a sequence length above 2 s.d. from the mean. MAFFT alignment was used to align the roughly 1,800 homologues that remained[38]. Because conservation is a limited domain, the L-INS-i iterative refinement method was used with a maxiterate 1,000 set. FastTree2 was used to compute an approximate maximum-likelihood phylogenetic tree. Available metadata associated with the proteins were used to classify hits as plasmid, phage or MAG. Proteins without associated metadata were included but not classified. Visualization was done with iTol and custom scripts were used to generate additional display features[39].

Protein structure

The predicted structures of AcrVA2 and FinQ were created by the AlphaFold Monomer (v2.0) pipeline and downloaded from AlphaFold DB (AcrVA2, AF-A0A7M4DUH0-F1-v4; FinQ, AF-E9LMI3-F1-v4)[8–10,40]. The structures of AcrVA2 with 30-amino-acid peptides from MbCas12a(58069), MbCas12a(33362) and LbCas12a(ND2006) were predicted using AlphaFold3 (ref. 10). All structures were visualized and analysed in PyMOL and ChimeraX.

Protein alignment

The protein sequences of different orthologues of AcrVA2 were aligned with Clustal Omega and coloured in Jalview using BLOSUM62 scheme.

Reporting summary

Further information on research design is available in the Nature Portfolio Reporting Summary linked to this article.

Data availability

Transcriptomic data have been deposited in the NCBI Sequence Read Archive under BioProject accession PRJNA1001058. The proteins used to construct the phylogenetic tree (https://doi.org/10.6084/m9.figshare.31680328) and the mass spectrometry data (https://doi.org/10.6084/m9.figshare.31680478) are publicly available on Figshare[41,42]. Uncropped images of gels and blots are presented in Supplementary Fig. 1. Source data are provided for Figs. 1c,d and 2i,l and Extended Data Figs. 1c, 2a–d, 4a,b, 5a,b and 9c,d. Amino acid alignments of AcrVA2 homologues are publicly available on Figshare (https://doi.org/10.6084/m9.figshare.31684630)[43]. Sequences of AcrVA2 homologues used to generate these amino acid alignments are listed in Supplementary Table 2. Nucleotide alignments of different *cas12a* variants downregulated by AcrVA2 are publicly available on Figshare (https://doi.org/10.6084/m9.figshare.31684813)[44]. Source data are provided with this paper.

Code availability

This paper does not report any original code.

29. Watters, K. E., Fellmann, C., Bai, H. B., Ren, S. M. & Doudna, J. A. Systematic discovery of natural CRISPR-Cas12a inhibitors. *Science* **362**, 236–239 (2018).
30. Hoang, T. T., Kutchma, A. J., Becher, A. & Schweizer, H. P. Integration-proficient plasmids for *Pseudomonas aeruginosa*: site-specific integration and use for engineering of reporter and expression strains. *Plasmid* **43**, 59–72 (2000).
31. Choi, K.-H. & Schweizer, H. P. mini-Tn7 insertion in bacteria with single attTn7 sites: example *Pseudomonas aeruginosa*. *Nat. Protoc.* **1**, 153–161 (2006).
32. Choi, K.-H., Kumar, A. & Schweizer, H. P. A 10-min method for preparation of highly electrocompetent *Pseudomonas aeruginosa* cells: application for DNA fragment transfer between chromosomes and plasmid transformation. *J. Microbiol. Methods* **64**, 391–397 (2006).
33. Peters, J. M. et al. Enabling genetic analysis of diverse bacteria with Mobile-CRISPRi. *Nat. Microbiol.* **4**, 244–250 (2019).
34. Sambrook, J. & Russell, D. *Molecular Cloning: A Laboratory Manual* 3rd edn (Cold Spring Harbor Laboratory, 2000).
35. Cox, J. & Mann, M. MaxQuant enables high peptide identification rates, individualized p.p.b.-range mass accuracies and proteome-wide protein quantification. *Nat. Biotechnol.* **26**, 1367–1372 (2008).
36. Teo, G. et al. SAINTexpress: improvements and additional features in Significance Analysis of INTeractome software. *J. Proteomics* **100**, 37–43 (2014).
37. Altschul, S. F. et al. Gapped BLAST and PSI-BLAST: a new generation of protein database search programs. *Nucleic Acids Res.* **25**, 3389–3402 (1997).
38. Katoh, K., Kuma, K.-I., Toh, H. & Miyata, T. MAFFT version 5: improvement in accuracy of multiple sequence alignment. *Nucleic Acids Res.* **33**, 511–518 (2005).
39. Letunic, I. & Bork, P. Interactive Tree Of Life (iTOL) v5: an online tool for phylogenetic tree display and annotation. *Nucleic Acids Res.* **49**, W293–W296 (2021).
40. Jumper, J. et al. Highly accurate protein structure prediction with AlphaFold. *Nature* **596**, 583–589 (2021).
41. Marino, N. Proteins — phylogenetic free. *Figshare* https://doi.org/10.6084/m9.figshare.31680328.v1 (2026).
42. Marino, N. Mass spectrometry results for AcrVA2 immunoprecipitation. *Figshare* https://doi.org/10.6084/m9.figshare.31680478.v1 (2026).
43. Marino, N. Alignment of AcrVA2 homologs. *Figshare* https://doi.org/10.6084/m9.figshare.31684630.v1 (2026).
44. Marino, N. Alignment of cas12a nucleotide sequences downregulated by AcrVA2. *Figshare* https://doi.org/10.6084/m9.figshare.31684813.v1 (2026).

Acknowledgements We thank members of the Bondy-Denomy laboratory and C. Gross laboratory for thoughtful discussions; K. Watters for providing plasmids; J. Peters and A. Buskirk for reagents and technical advice; M. Paredes and D. Le for preparing the media used in this work; and K. Lynch for providing us with the necessary facilities and equipment to perform radioactivity experiments. Sequencing was performed at the UCSF CAT. This work was supported by the US National Institutes of Health (R01GM127489), the Vallee Foundation and the Searle Scholarship, and the Defense Advanced Research Projects Agency (DARPA) award HR0011-17-2-0043. The views, opinions and/or findings expressed are those of the authors and should not be interpreted as representing the official views or policies of the Department of Defense or the DARPA Safe Genes program (HR0011-17-2-0043). N.D.M. was supported by the National Institutes of Health awards F32GM133127, K99GM143476 and R00GM143476. M.G. was funded by the Federal Ministry of Research, Technology and Space of Germany under the Microbial Stargazing project (ref. 01KX2324). J.V. was supported by the Gottfried Wilhelm

Leibniz Award (DFG Vo875-18) and SPP2330 (DFG Vo875-23/2). J.V. is a member of the DFG Cluster of Excellence NUCLEATE for Nucleic Acid Sciences and Technologies (Project-ID 533767322 – EXC 3113/1).

Author contributions N.D.M. and J.B.-D. conceptualized the project. N.D.M., M.G., A.D.S., A.F.T., K.Z., S.S., M.C.J. and D.L.S. contributed to the experimental design. N.D.M. and J.B.-D. acquired funding. N.D.M. performed the plasmid construction, strain engineering, phage plaque assays, western blots, immunoprecipitations, qRT–PCR, northern blots, RNA sequencing library preparation, growth assays, and structural and sequence alignments. A.T. performed the plasmid construction, strain engineering, in vitro cleavage assays, qRT–PCR, western blots and plaque assays. M.G. and L.B. performed the sucrose gradients and western blots. J.L.R. performed the plasmid construction, strain engineering, northern blots, western blots and growth assays. A.D.S. performed the plasmid construction, strain engineering, western blots and qRT–PCR. A.F.T. and K.Z. performed the northern and western blots. H.C. performed the immunoprecipitations and western blots. T.J.A. performed the plaque assays, western blots and qRT–PCR. J.L. performed the strain engineering, plaque assays, western blots and nucleotide alignments. S.H. performed the strain engineering and plaque assays. M.C.J. generated the phylogenetic tree. S.S. performed the RNA sequencing analysis. L.Y. plotted the transcriptomics data. K.-H.C. performed the liquid chromatography–mass spectrometry and analysis. Y.Z. performed the protein purification and in vitro assays. N.D.M., J.B.-D., J.V., M.G. and D.L.S. oversaw the different aspects of the project. N.D.M. and J.B.-D. wrote the manuscript with input from all authors.

Competing interests The UCSF has filed a patent on the use of inhibitors of CRISPR–Cas12a, on which N.D.M. and J.B.-D. are listed as inventors. J.B.-D. is a scientific advisory board member of SNIPR Biome and Excision Biotherapeutics, a consultant to LeapFrog Bio, and a scientific advisory board member and co-founder of Acrigen Biosciences. The Bondy-Denomy laboratory received research support from Felix Biotechnology. The other authors declare no competing interests.

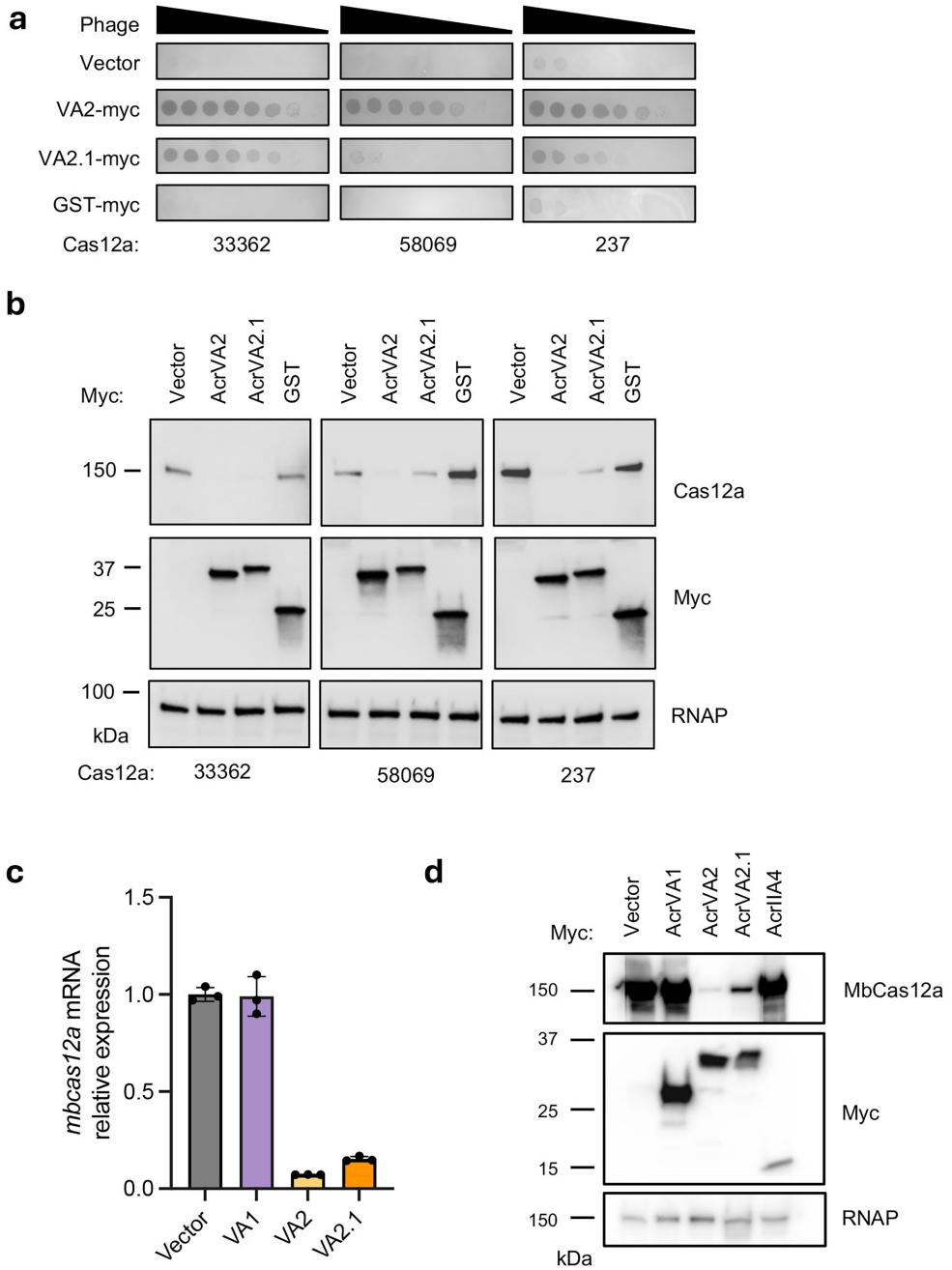
Additional information

Supplementary information The online version contains supplementary material available at https://doi.org/10.1038/s41586-026-10440-8.

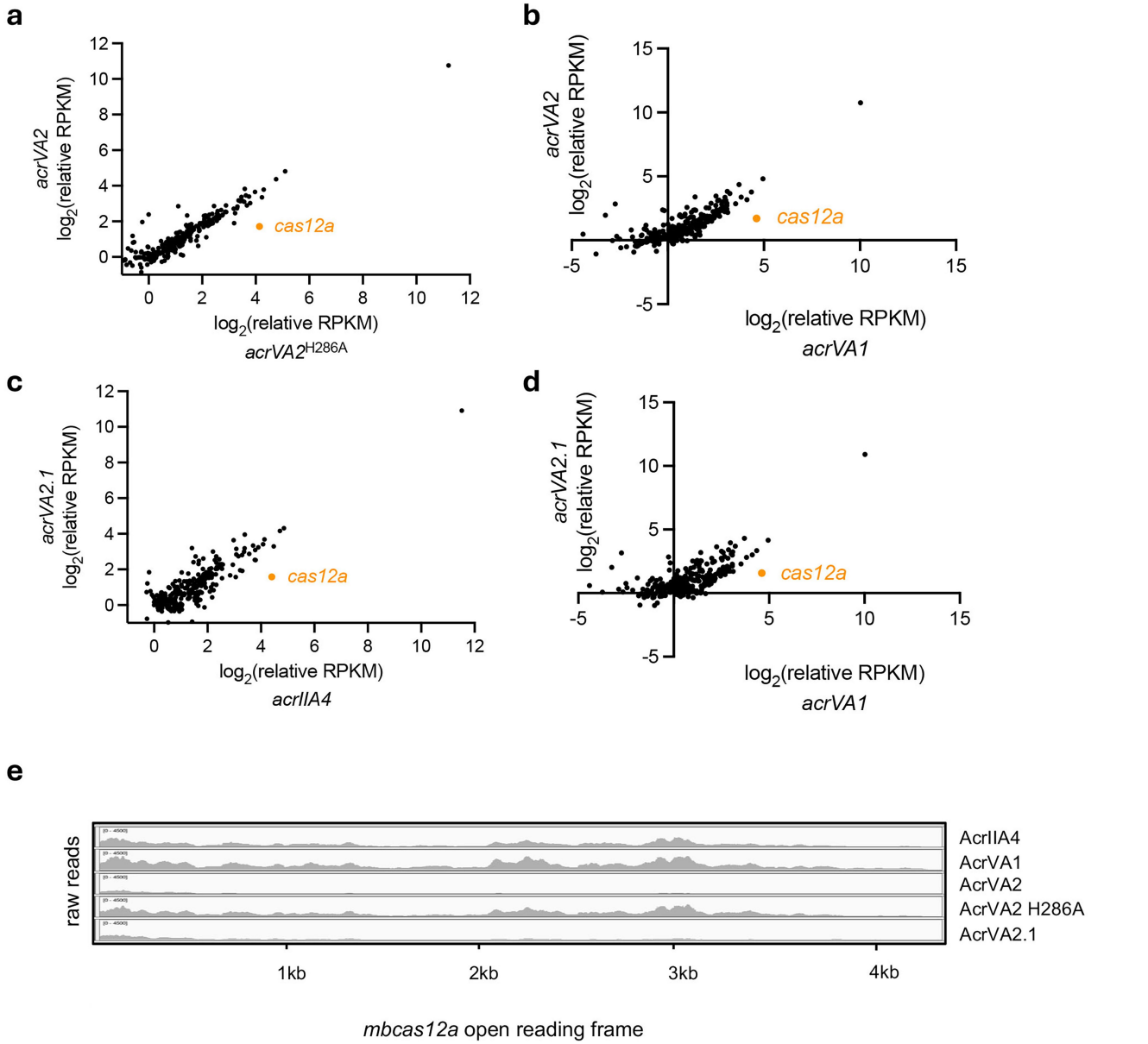
Correspondence and requests for materials should be addressed to Nicole D. Marino or Joseph Bondy-Denomy.

Peer review information *Nature* thanks John van der Oost and the other, anonymous, reviewer(s) for their contribution to the peer review of this work.

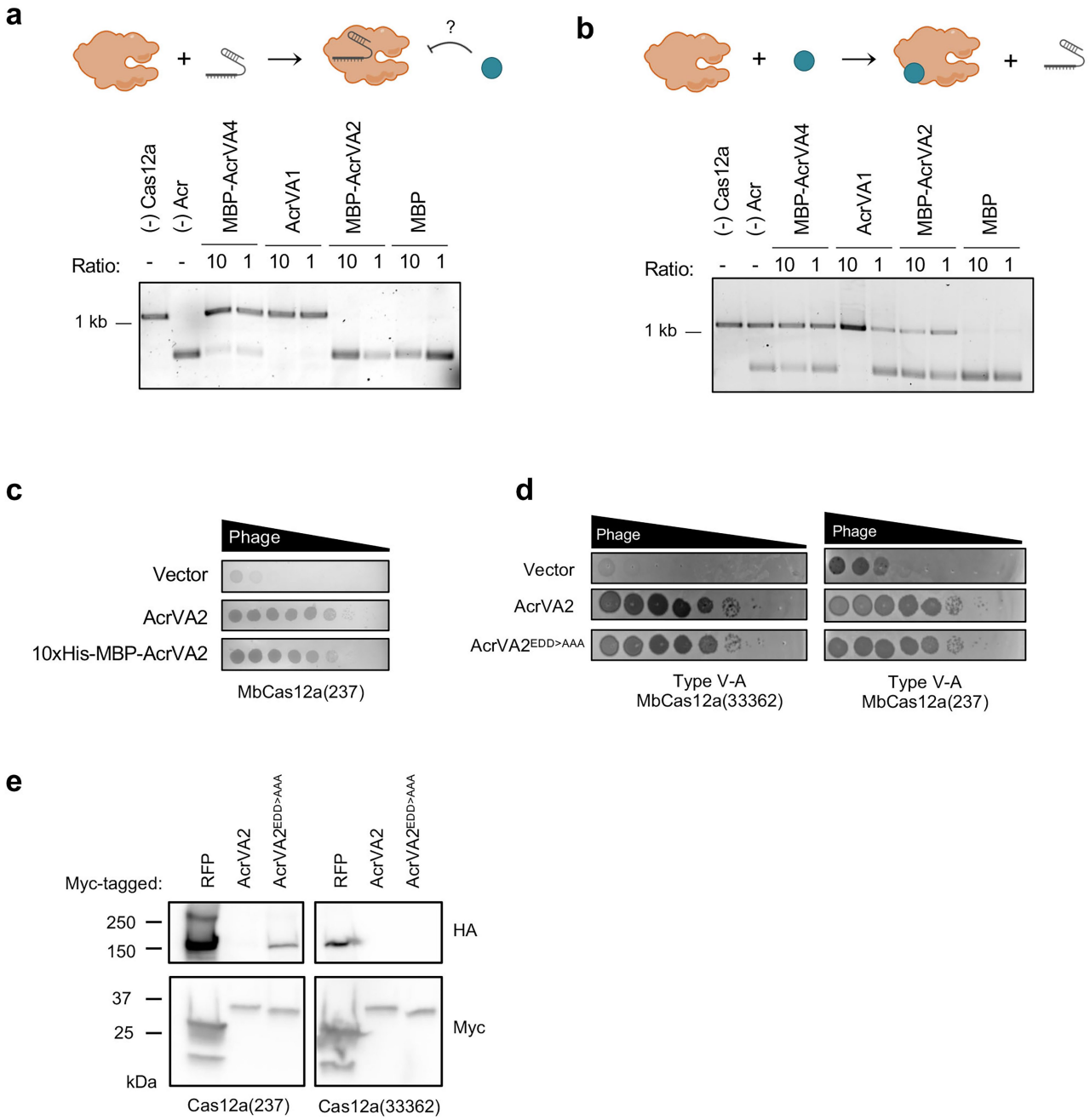
Reprints and permissions information is available at http://www.nature.com/reprints.



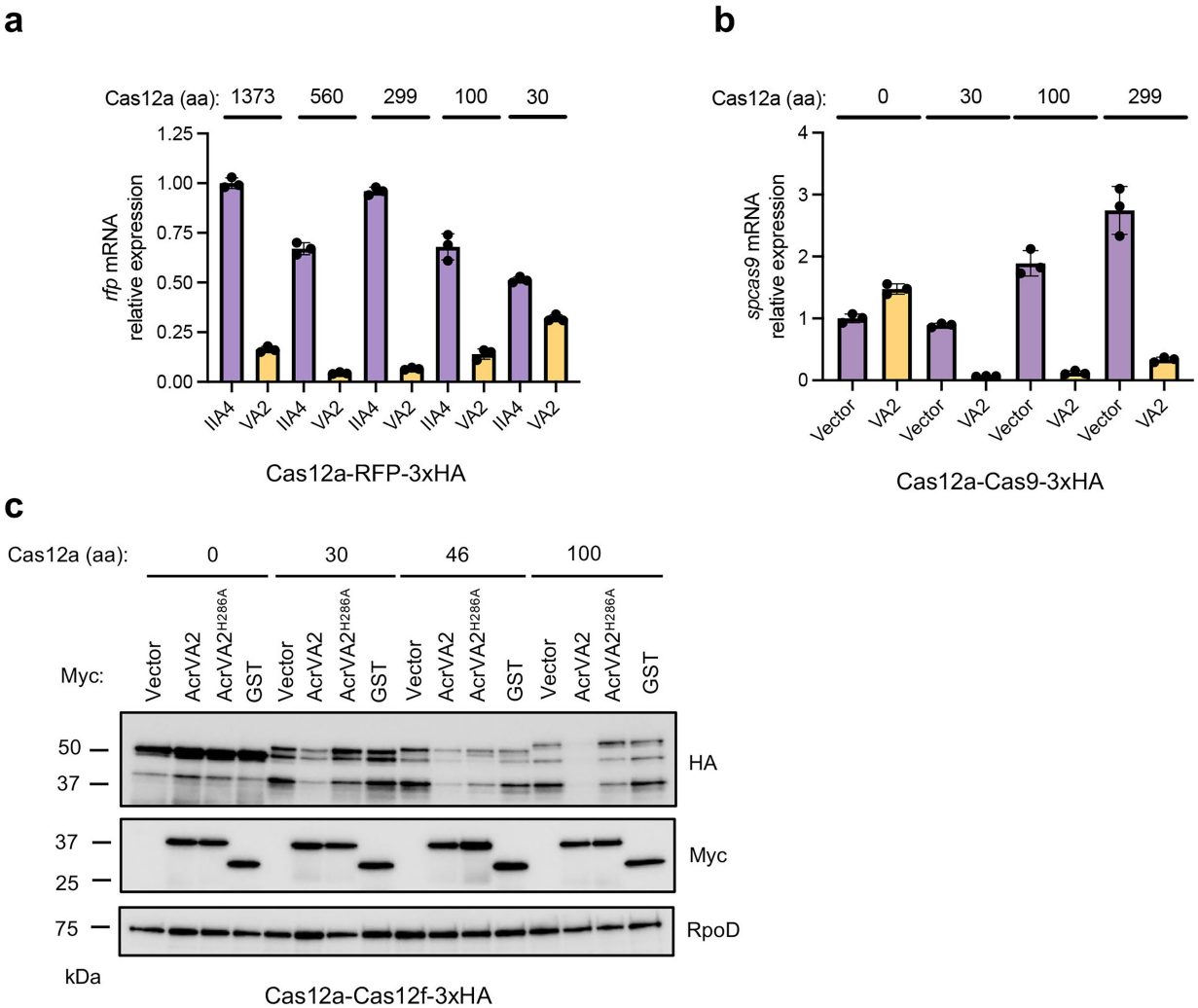
Extended Data Fig. 1 | AcrVA2 inhibits and downregulates diverse variants of *cas12a*. (**a**) Phage plaque assay using ten-fold serial dilution of phage to assess Cas12a inhibition by AcrVA2 (or homolog AcrVA2.1) compared to controls. 33362, 237, and 58069 refer to the *Moraxella bovoculi* strains that encode the corresponding Cas12a homolog. (**b**) Western blot on bacterial lysates to assess the effect of myc-tagged AcrVA2 or control proteins on Cas12a-3xHA expression. 33362, 237, and 58069 refer to the *Moraxella bovoculi* strains that encode each Cas12a ortholog. RNAP, RNA polymerase (loading control). (**c**) Codon-modified *mbcas12a* mRNA levels were quantified by qRT-PCR and normalized to *rpoD*. Expression is shown relative to empty vector control using the ΔΔCt method. Points represent technical triplicates ($n = 3$ technical replicates) from one representative experiment; mean ± standard deviation indicated. (**d**) Western blot on bacterial lysates to assess downregulation of codon-modified HA-tagged MbCas12a by myc-tagged AcrVA2 and AcrVA2.1 relative to controls. RNAP, RNA polymerase (loading control). Experiments in (a–d) were independently repeated at least twice with similar results.



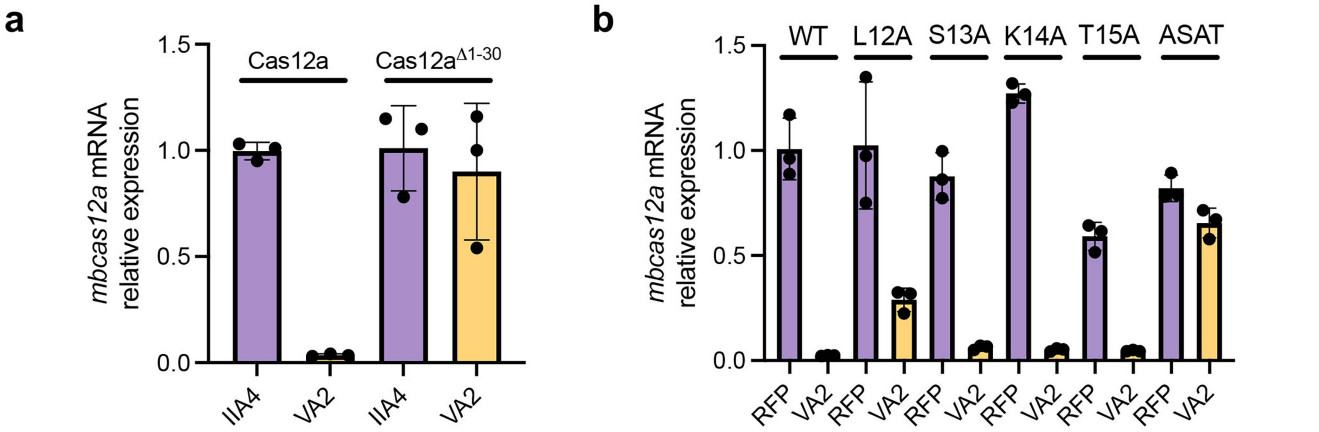
Extended Data Fig. 2 | Comparative transcriptomic analysis of bacteria expressing AcrVA2 and controls. (**a**–**d**) Gene expression was quantified as reads per kilobase per million mapped reads (RPKM), normalized to the housekeeping gene *rpoD*, and $\log_2$-transformed. Each point represents one gene. The diagonal line denotes equal expression between samples. (**e**) Raw read coverage is shown across the full *mbcas12a* open reading frame, with read depth indicating transcript abundance at each position. The mapping was performed using standard RNA-seq alignment workflows, and raw coverage profiles are presented without normalization to highlight differences in expression levels between samples. Reads Per Kilobase of transcript per Million mapped reads (RPKM) values for *mbcas12a* are as indicated for each sample: AcrIIA4, 217; AcrVA1, 316; AcrVA2, 38; AcrVA2 H286A, 225; AcrVA2.1, 71. Samples were processed simultaneously, and the experiment was not repeated.



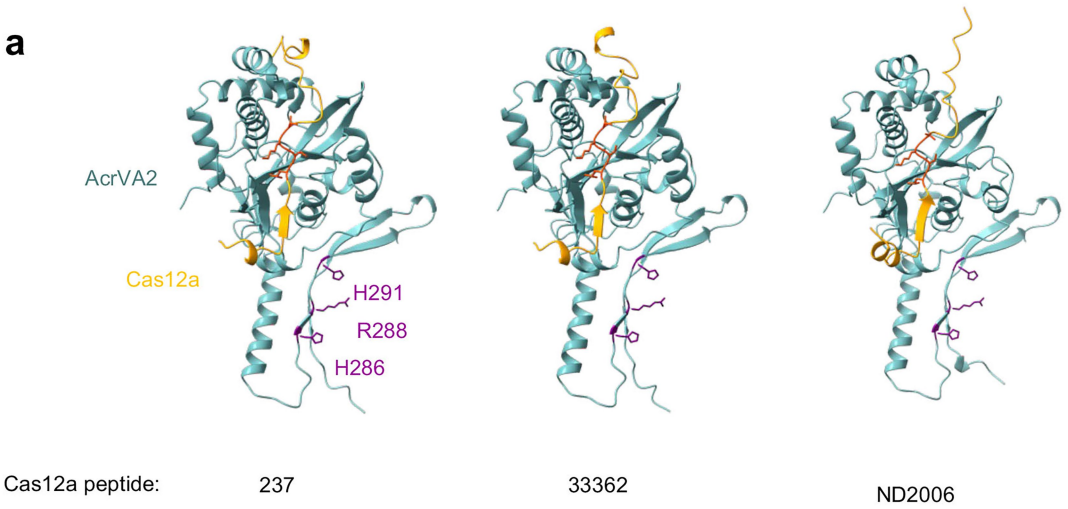
Extended Data Fig. 3 | AcrVA2 does not inhibit or downregulate *cas12a* in vitro. (**a**) In vitro cleavage assay with purified anti-CRISPR protein added to MbCas12a(33362) ribonucleoprotein complexes programmed to target a double-stranded DNA amplicon. Cas12a and crRNA were assembled into ribonucleoprotein complexes *before* addition of anti-CRISPR or control. Anti-CRISPR or control protein was added at a 1:10 or 1:1 ratio relative to Cas12a. (**b**) In vitro cleavage assay with purified anti-CRISPR protein added to apoMbCas12a(33362) *before* addition of crRNA and target dsDNA. Anti-CRISPR or control protein was added in a 10:1 or 1:1 ratio relative to apoCas12a. (**c**) Phage plaque assay using ten-fold serial dilution of phage to assess Cas12a inhibition by 10xHis-MBP-AcrVA2 relative to AcrVA2 and vector control. (**d**) Phage plaque assay on strains expressing different homologs of *mbcas12a* from *M. bovoculi* strains 237 and 33362. Ten-fold serial dilutions of phage were plated on bacterial lawns to assess Cas12a inhibition. (**e**) Western blot on bacterial lysates to assess downregulation of different *mbcas12* orthologs by AcrVA2 E98A/D129A/D195A relative to controls. Experiments in (a–e) were independently repeated at least twice with similar results.



Extended Data Fig. 4 | Fusing the N-terminal polypeptide of Cas12a to other proteins enables their downregulation. (**a**) mRNA levels were quantified for *cas12a-rfp* fusions and normalized to *rpoD*. Numbers refer to the amino acid length of Cas12a fused to RFP-3xHA. Expression is shown relative to samples encoding full-length *cas12a* with *acrIIA4* control using the ΔΔCt method. (**b**) mRNA levels were quantified for *cas12a-cas9* fusions by qRT-PCR and normalized to *rpoD*. Expression is shown relative to samples with *cas9* empty vector control using the ΔΔCt method. For both (a) and (b), points represent technical triplicates ($n = 3$ technical replicates) from one representative qRT-PCR experiment; mean ± standard deviation indicated. (**c**) Western blot on bacterial lysates to assess effect of AcrVA2-myc or controls on Cas12a-Cas12f fusions. For (a–c), numbers indicate length of truncated Cas12a polypeptide in amino acids. RpoD, loading control. All experiments were independently repeated at least twice with similar results.



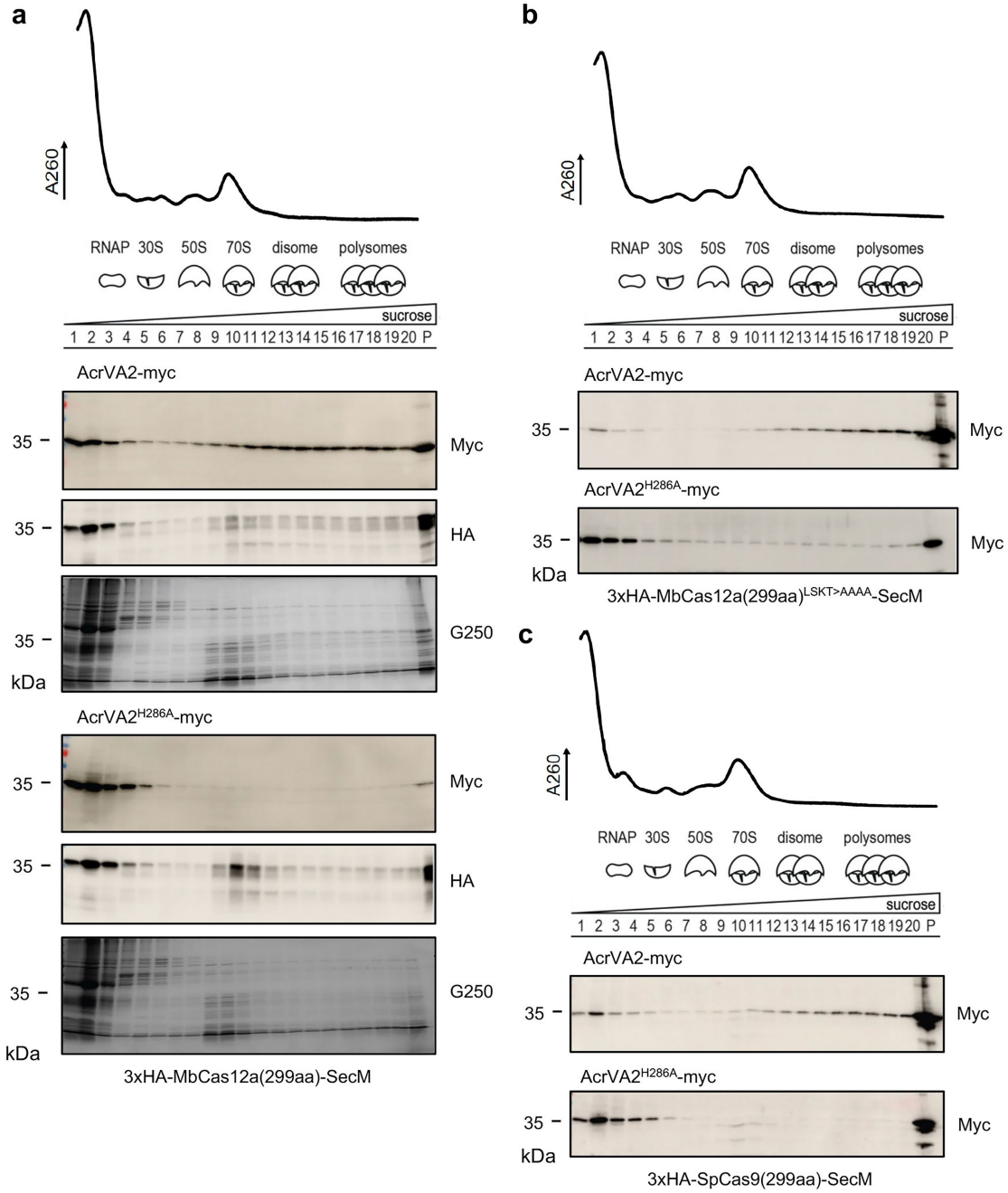
Extended Data Fig. 5 | Cas12a N-terminal amino acids are required for mRNA degradation by AcrVA2. (**a**) mRNA levels were quantified for wildtype *cas12a* and mutant *cas12a* lacking the first 30 amino acids (but provided with a start codon) and normalized to *rpoD*. Expression is shown relative to *acrIIA4* control. (**b**) RNA levels were quantified for wildtype and mutant *cas12a* and normalized to *rpoD*. Expression is shown relative to *rfp* control. For both (a) and (b), points represent technical triplicates ($n = 3$ technical replicates) from one representative qRT-PCR experiment calculated using the ΔΔCt method; mean ± standard deviation indicated. Each experiment was independently repeated at least twice with similar results.



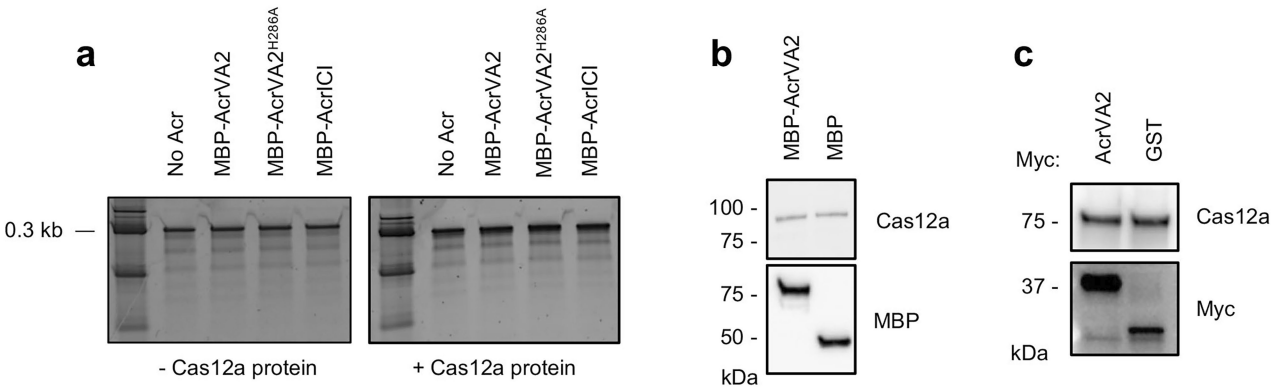
b

237	--MLFQDFTHLYPLSKTVRFELKPIDRTLEHI
33362	--MLFQDFTHLYPLSKTVRFELKPIGKTLEHI
ND2006	AASKLEKFTNCYSLSKTLRFKAIPVGKTQE--

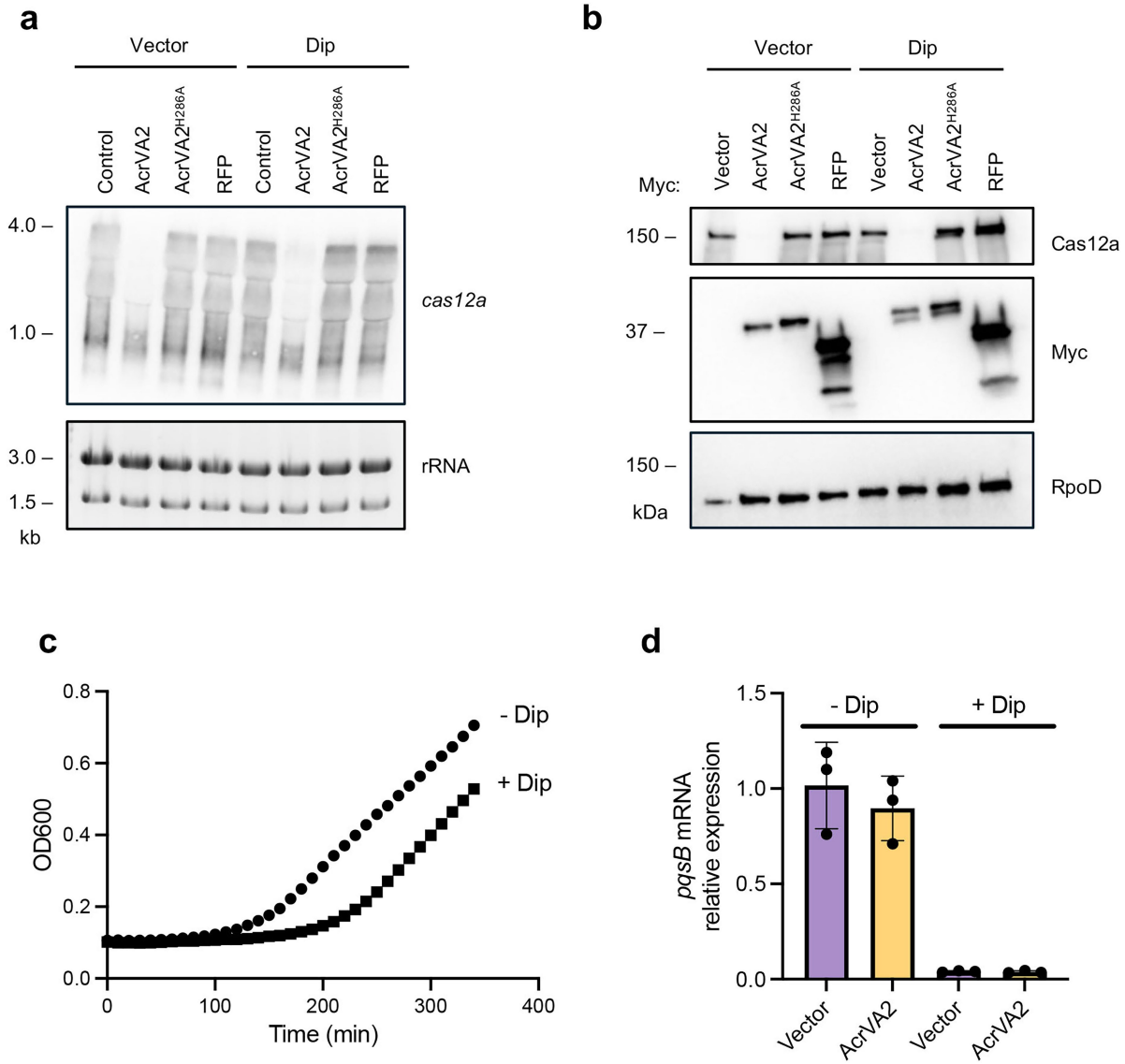
Extended Data Fig. 6 | Predicted structures of AcrVA2 and Cas12a polypeptide. (**a**) Predicted AlphaFold structures of AcrVA2 (teal) with 30 amino acid polypeptides (yellow) from *Moraxella bovoculi* strains 237 and 33362 and *Lachnospiraceae bacterium* ND2006. LSKT amino acids (red) in Cas12a and H286, R288, and H291 (purple) in AcrVA2 are indicated. (**b**) Polypeptide sequences of Cas12a from *Moraxella bovoculi* strains 237 and 33362 and *Lachnospiraceae bacterium* ND2006.



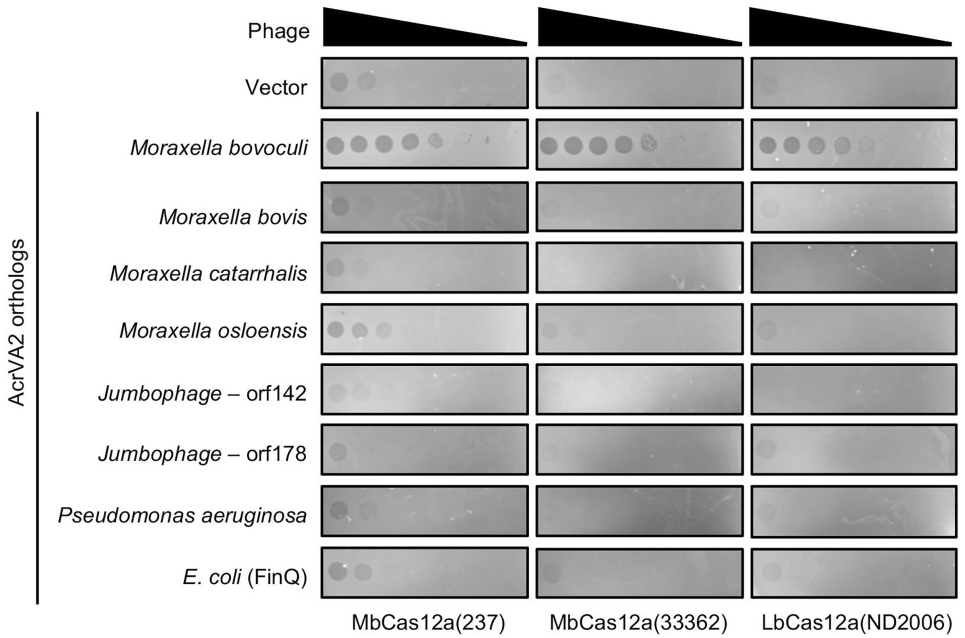
Extended Data Fig. 7 | AcrVA2 co-fractionates with ribosomes and polysomes independently of Cas12a. (**a**) Sedimentation profiles and protein analysis were performed on lysate samples (1–20) collected after separation on a sucrose gradient. Bacteria were engineered and induced to co-express 3xHA-MbCas12a(299aa)-SecM with AcrVA2-myc or AcrVA2^{H286A}-myc. Western blots were performed on samples using anti-Myc and anti-HA antibodies. Coomassie G-250 was used to stain total protein. Images indicate gene expression machinery enriched in different fractions based on A260 traces, total protein stain, and mass spectrometry analysis. (**b**) Western blot for AcrVA2-myc on fractions (1–20) collected after lysates were separated on a sucrose gradient. Bacteria were engineered and induced to co-express 3xHA-MbCas12a(299aa)$^{LSKT>AAAA}$-SecM with AcrVA2-myc or AcrVA2^{H286A}-myc. Images indicate gene expression machinery enriched in different fractions. (**c**) Western blot for AcrVA2-myc on lysate samples (1–20) collected after separation on a sucrose gradient. Bacteria were engineered and induced to co-express 3xHA-SpCas9(299aa)-SecM with AcrVA2-myc or AcrVA2^{H286A}-myc. Images indicate gene expression machinery enriched in different fractions. Experiments were independently repeated at least twice with similar results.



Extended Data Fig. 8 | AcrVA2 does not downregulate *cas12a* directly in vitro. (**a**) Purified MBP-AcrVA2 protein or controls were incubated with *mbcas12a* mRNA in vitro with or without purified MbCas12a(33362) protein added in trans. Samples were resolved on a TBE-urea gel and strained with SYBR gold. AcrIC1 is a type I-C CRISPR-Cas inhibitor that does not inhibit Cas12a. (**b**) Purified MBP-AcrVA2 or MBP control proteins were added to PURE transcription-translation reactions in which Cas12a(560aa)-RFP-3xHA was expressed from a linear DNA template. Reactions were resolved on SDS-PAGE and probed by Western blot. MBP, maltose binding protein. (**c**) Western blot on PURE transcription-translation reactions in which Cas12a(560aa)-RFP-3xHA was co-expressed with AcrVA2-myc or GST-myc expressed from linear DNA templates. Glutathione S-transferase (GST) was used as a control. Experiments were independently repeated at least twice with similar results.



Extended Data Fig. 9 | RNase E is not required for *cas12a* mRNA degradation by AcrVA2. (**a**) Northern blot on *mbcas12a* mRNA co-expressed with AcrVA2 and Dip or vector controls in bacteria. Ribosomal RNA (rRNA) included as a loading control. (**b**) Western blot on bacterial lysates harvested from the same experiment as (a). (**c**) Growth assay on bacteria expressing MbCas12a and Dip or vector control. Time indicates minutes after subculture and Dip induction. (**d**) mRNA levels were quantified for *pqsB* by qRT-PCR and normalized to *rpoD*. Expression is shown relative to samples with vector control using the ΔΔCt method. Points represent technical triplicates ($n = 3$ technical replicates) from one representative experiment; mean ± standard deviation indicated. Experiments in (a–d) were independently repeated at least twice with similar results.



Extended Data Fig. 10 | AcrVA2 orthologs from other bacterial species do not inhibit Cas12a. Phage plaque assay on strains expressing different orthologs of Cas12a and AcrVA2. Ten-fold serial dilutions of phage were plated on bacterial lawns to assess Cas12a inhibition. All plaque assays were repeated at least twice with similar results.

nature portfolio

Corresponding author(s): Nicole D. Marino and Joseph Bondy-Denomy

Last updated by author(s): 2023/06/25

Reporting Summary

Nature Portfolio wishes to improve the reproducibility of the work that we publish. This form provides structure for consistency and transparency in reporting. For further information on Nature Portfolio policies, see our Editorial Policies and the Editorial Policy Checklist.

Please do not complete any field with "not applicable" or n/a. Refer to the help text for what text to use if an item is not relevant to your study.
For final submission: please carefully check your responses for accuracy; you will not be able to make changes later.

Statistics

For all statistical analyses, confirm that the following items are present in the figure legend, table legend, main text, or Methods section.

n/a	Confirmed	
☐	☒	The exact sample size (*n*) for each experimental group/condition, given as a discrete number and unit of measurement
☐	☒	A statement on whether measurements were taken from distinct samples or whether the same sample was measured repeatedly
☒	☐	The statistical test(s) used AND whether they are one- or two-sided *Only common tests should be described solely by name; describe more complex techniques in the Methods section.*
☒	☐	A description of all covariates tested
☒	☐	A description of any assumptions or corrections, such as tests of normality and adjustment for multiple comparisons
☐	☒	A full description of the statistical parameters including central tendency (e.g. means) or other basic estimates (e.g. regression coefficient) AND variation (e.g. standard deviation) or associated estimates of uncertainty (e.g. confidence intervals)
☒	☐	For null hypothesis testing, the test statistic (e.g. *F*, *t*, *r*) with confidence intervals, effect sizes, degrees of freedom and *P* value noted *Give P values as exact values whenever suitable.*
☒	☐	For Bayesian analysis, information on the choice of priors and Markov chain Monte Carlo settings
☒	☐	For hierarchical and complex designs, identification of the appropriate level for tests and full reporting of outcomes
☒	☐	Estimates of effect sizes (e.g. Cohen's *d*, Pearson's *r*), indicating how they were calculated

Our web collection on statistics for biologists contains articles on many of the points above.

Software and code

Policy information about availability of computer code

Data collection	No original code was used in this study.
Data analysis	No original code was used in this study.

For manuscripts utilizing custom algorithms or software that are central to the research but not yet described in published literature, software must be made available to editors and reviewers. We strongly encourage code deposition in a community repository (e.g. GitHub). See the Nature Portfolio guidelines for submitting code & software for further information.

Data

Policy information about availability of data

All manuscripts must include a data availability statement. This statement should provide the following information, where applicable:

- Accession codes, unique identifiers, or web links for publicly available datasets
- A description of any restrictions on data availability
- For clinical datasets or third party data, please ensure that the statement adheres to our policy

Transcriptomic data have been deposited in the NCBI Sequence Read Archive (SRA) under BioProject accession PRJNA1433509

Research involving human participants, their data, or biological material

Policy information about studies with human participants or human data. See also policy information about sex, gender (identity/presentation), and sexual orientation and race, ethnicity and racism.

Reporting on sex and gender	N/A
Reporting on race, ethnicity, or other socially relevant groupings	N/A
Population characteristics	N/A
Recruitment	N/A
Ethics oversight	N/A

Note that full information on the approval of the study protocol must also be provided in the manuscript.

Field-specific reporting

Please select the one below that is the best fit for your research. If you are not sure, read the appropriate sections before making your selection.

☒ Life sciences ☐ Behavioural & social sciences ☐ Ecological, evolutionary & environmental sciences

For a reference copy of the document with all sections, see nature.com/documents/nr-reporting-summary-flat.pdf

Life sciences study design

All studies must disclose on these points even when the disclosure is negative.

Sample size	Technical triplicates (n=3) were used for quantitative analysis (mean and standard deviation).
Data exclusions	No data were excluded.
Replication	Representative experiments were repeated at least twice using independent colonies over multiple experiments with similar results.
Randomization	Random colonies were selected from the plate for each experiment. Colonies are derived from specific strain engineering efforts and can not be randomized further.
Blinding	No blinding was done in this study, since the effect sizes (generally 10x or more) were large enough to not warrant blinding and are immediately visible (in Western blots, plaque assays, etc).

Behavioural & social sciences study design

All studies must disclose on these points even when the disclosure is negative.

Study description	N/A
Research sample	N/A
Sampling strategy	N/A
Data collection	N/A
Timing	N/A
Data exclusions	N/A
Non-participation	N/A
Randomization	N/A

Ecological, evolutionary & environmental sciences study design

All studies must disclose on these points even when the disclosure is negative.

Study description	N/A
Research sample	N/A
Sampling strategy	N/A
Data collection	N/A
Timing and spatial scale	N/A
Data exclusions	N/A
Reproducibility	N/A
Randomization	N/A
Blinding	N/A

Did the study involve field work? ☐ Yes ☒ No

Field work, collection and transport

Field conditions	
Location	
Access & import/export	
Disturbance	

Reporting for specific materials, systems and methods

We require information from authors about some types of materials, experimental systems and methods used in many studies. Here, indicate whether each material, system or method listed is relevant to your study. If you are not sure if a list item applies to your research, read the appropriate section before selecting a response.

Materials & experimental systems

n/a	Involved in the study
☐	☒ Antibodies
☒	☐ Eukaryotic cell lines
☒	☐ Palaeontology and archaeology
☒	☐ Animals and other organisms
☒	☐ Clinical data
☒	☐ Dual use research of concern
☒	☐ Plants

Methods

n/a	Involved in the study
☒	☐ ChIP-seq
☒	☐ Flow cytometry
☒	☐ MRI-based neuroimaging

Antibodies

Antibodies used	anti-Myc, anti-HA, anti-RpoD, anti-RNAP, anti-LbCas12a, anti-SpyCas9
Validation	We tested antibodies against strains lacking target (where possible) and confirmed size of targeted protein.

Eukaryotic cell lines

Policy information about cell lines and Sex and Gender in Research

Cell line source(s)	
Authentication	
Mycoplasma contamination	
Commonly misidentified lines (See ICLAC register)	

Palaeontology and Archaeology

Specimen provenance	
Specimen deposition	
Dating methods	

☐ Tick this box to confirm that the raw and calibrated dates are available in the paper or in Supplementary Information.

Ethics oversight	

Note that full information on the approval of the study protocol must also be provided in the manuscript.

Animals and other research organisms

Policy information about studies involving animals; ARRIVE guidelines recommended for reporting animal research, and Sex and Gender in Research

Laboratory animals	
Wild animals	
Reporting on sex	
Field-collected samples	
Ethics oversight	

Note that full information on the approval of the study protocol must also be provided in the manuscript.

Clinical data

Policy information about clinical studies

All manuscripts should comply with the ICMJE guidelines for publication of clinical research and a completed CONSORT checklist must be included with all submissions.

Clinical trial registration	
Study protocol	
Data collection	
Outcomes	

Dual use research of concern

Policy information about dual use research of concern

Hazards

Could the accidental, deliberate or reckless misuse of agents or technologies generated in the work, or the application of information presented in the manuscript, pose a threat to:

No	Yes	
☐	☐	Public health
☐	☐	National security
☐	☐	Crops and/or livestock
☐	☐	Ecosystems
☐	☐	Any other significant area

Experiments of concern

Does the work involve any of these experiments of concern:

No	Yes	
☐	☐	Demonstrate how to render a vaccine ineffective
☐	☐	Confer resistance to therapeutically useful antibiotics or antiviral agents
☐	☐	Enhance the virulence of a pathogen or render a nonpathogen virulent
☐	☐	Increase transmissibility of a pathogen
☐	☐	Alter the host range of a pathogen
☐	☐	Enable evasion of diagnostic/detection modalities
☐	☐	Enable the weaponization of a biological agent or toxin
☐	☐	Any other potentially harmful combination of experiments and agents

Plants

Seed stocks

Novel plant genotypes

Authentication

ChIP-seq

Data deposition

☐ Confirm that both raw and final processed data have been deposited in a public database such as GEO.

☐ Confirm that you have deposited or provided access to graph files (e.g. BED files) for the called peaks.

Data access links
May remain private before publication.

Files in database submission

Genome browser session
(e.g. UCSC)

Methodology

Replicates

Sequencing depth

Antibodies

Peak calling parameters

Data quality

Software

Flow Cytometry

Plots

Confirm that:

☐ The axis labels state the marker and fluorochrome used (e.g. CD4-FITC).

☐ The axis scales are clearly visible. Include numbers along axes only for bottom left plot of group (a 'group' is an analysis of identical markers).

☐ All plots are contour plots with outliers or pseudocolor plots.

☐ A numerical value for number of cells or percentage (with statistics) is provided.

Methodology

Sample preparation

Instrument

Software

Cell population abundance

Gating strategy

☐ Tick this box to confirm that a figure exemplifying the gating strategy is provided in the Supplementary Information.

Magnetic resonance imaging

Experimental design

Design type

Design specifications

Behavioral performance measures

Imaging type(s)

Field strength

Sequence & imaging parameters

Area of acquisition

Diffusion MRI ☐ Used ☐ Not used

Preprocessing

Preprocessing software

Normalization

Normalization template

Noise and artifact removal

Volume censoring

Statistical modeling & inference

Model type and settings

Effect(s) tested

Specify type of analysis: ☐ Whole brain ☐ ROI-based ☐ Both

Statistic type for inference

(See Eklund et al. 2016)

Correction

Models & analysis

n/a	Involved in the study
☐	☐ Functional and/or effective connectivity
☐	☐ Graph analysis
☐	☐ Multivariate modeling or predictive analysis

Functional and/or effective connectivity

Graph analysis

Multivariate modeling and predictive analysis

This checklist template is licensed under a Creative Commons Attribution 4.0 International License, which permits use, sharing, adaptation, distribution and reproduction in any medium or format, as long as you give appropriate credit to the original author(s) and the source, provide a link to the Creative Commons license, and indicate if changes were made. The images or other third party material in this article are included in the article's Creative Commons license, unless indicated otherwise in a credit line to the material. If material is not included in the article's Creative Commons license and your intended use is not permitted by statutory regulation or exceeds the permitted use, you will need to obtain permission directly from the copyright holder. To view a copy of this license, visit http://creativecommons.org/licenses/by/4.0/

